BIOCHEMISTRY
including biophysical chemistry & molecular biology

Article

pubs.acs.org/biochemistry

# Evidence of the Direct Involvement of the Substrate TCP Radical in Functional Switching from Oxyferrous $O_2$ Carrier to Ferric Peroxidase in the Dual-Function Hemoglobin/Dehaloperoxidase from *Amphitrite ornata*

Shengfang Sun,[†] Masanori Sono,*[,†] Jing Du,[†,§] and John H. Dawson*[,†,‡]

[†]Department of Chemistry and Biochemistry, University of South Carolina, Columbia, South Carolina 29208, United States
[‡]School of Medicine, University of South Carolina, Columbia, South Carolina 29208, United States

Supporting Information

**ABSTRACT:** The coelomic $O_2$-binding hemoglobin dehaloperoxidase (DHP) from the sea worm *Amphitrite ornata* is a dual-function heme protein that also possesses a peroxidase activity. Two different starting oxidation states are required for reversible $O_2$ binding (ferrous) and peroxidase (ferric) activity, bringing into question how DHP manages the two functions. In our previous study, the copresence of substrate 2,4,6-trichlorophenol (TCP) and $H_2O_2$ was found to be essential for the conversion of oxy-DHP to enzymatically active ferric DHP. On the basis of that study, a functional switching mechanism involving substrate radicals (TCP$^\bullet$) was proposed. To further support this mechanism, herein we report details of our investigations into the $H_2O_2$-mediated conversion of oxy-DHP to the ferric or ferryl ([TCP] < [$H_2O_2$]) state triggered by both biologically relevant [TCP and 4-bromophenol (4-BP)] and nonrelevant (ferrocyanide) compounds. At <50 $\mu$M $H_2O_2$, all of these conversion reactions are completely inhibited by ferric heme ligands (KCN and imidazole), indicating the involvement of ferric DHP. Furthermore, the spin-trapping reagent 5,5-dimethyl-1-pyrroline-*N*-oxide (DMPO) effectively inhibits the TCP/4-BP (but not ferrocyanide)-triggered conversion of oxy-DHP to ferric DHP. These results and $O_2$ concentration-dependent conversion rates observed in this study demonstrate that substrate TCP triggers the conversion of oxy-DHP to a peroxidase by TCP$^\bullet$ oxidation of the deoxyferrous state. TCP$^\bullet$ is progressively generated, by increasingly produced amounts of ferric DHP, upon $H_2O_2$ oxidation of TCP catalyzed initially by trace amounts of ferric enzyme present in the oxy-DHP sample. The data presented herein further address the mechanism of how the halophenolic substrate triggers the conversion of hemoglobin DHP into a peroxidase.

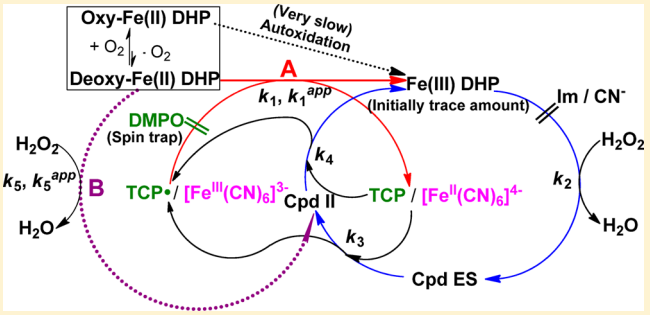


Dehaloperoxidase (DHP) from the terebellid polychaete *Amphitrite ornata* is a dual-functional dioxygen-binding hemoglobin that also exhibits peroxidase activity. As the most abundant protein in this worm,[1] DHP mainly functions as an $O_2$ carrier globin. It is isolated in the oxyferrous state[1] and has a moderate $O_2$ affinity ($K_{O_2}$) at 5.1−7.7 $\mu$M (22 °C).[2,3] As a peroxidase, ferric DHP catalyzes the $H_2O_2$-dependent oxidative dehalogenation of 2,4,6-trihalophenol (TXP) substrates to the corresponding 2,6-dihaloquinones (DXQ) (where X = Cl and Br), providing *A. ornata* with protection against toxic halophenols that are excreted by another inhabitant, *Notomastus lobatus*, in its living environment.[4,5] The dehaloperoxidase reaction mechanism is similar to that of horseradish peroxidase (HRP)-catalyzed or chloroperoxidase (CPO)-catalyzed oxidation that involves two consecutive one-electron oxidations of TXP to TXP radical by two high-valent (ferryl) oxidants Cpd I/Cpd ES and Cpd II (Scheme 1).[6−12] The TXP radicals generated in the catalytic cycle then form the final product DXQ, possibly by either disproportionation or by further enzymatic one-electron oxidation of the radicals, followed by hydration.[13,14] Kinetic studies have shown that at pH 5.4, DHP catalyzes dechlorination of 2,4,6-trichlorophenol (TCP) at rates ($k_{cat}$) ~33 times slower than that of HRP but ~13 times faster than that of myoglobin (Mb).[4,15] The moderate peroxidase activity of DHP arises from several structural adaptations it has acquired during its evolution from an ancient $O_2$ carrier with its proximal neutral histidine conserved.[3,16−18] Besides TXP, the much less toxic monohalophenols (4-XP) are copresent in the *A. ornata* ecosystem.[19,20] Although 4-bromophenol (4-BP) is apparently a competitive inhibitor for substrate TCP catalysis,[21] it has been recently shown that 4-BP itself is also oxidized by DHP with slow yet measurable turnover.[22] DHP has two isozyme forms, DHP A and DHP B, encoded by two separate genes. They have

**Received:** March 5, 2014
**Revised:** June 25, 2014
**Published:** June 27, 2014

   dx.doi.org/10.1021/bi5002757 | *Biochemistry* 2014, 53, 4956−4969

**Scheme 1. Catalytic Cycle for the Peroxidase-Catalyzed Oxidative Dehalogenation of 2,4,6-Trihalophenol (TXP) (adapted from ref 6)**

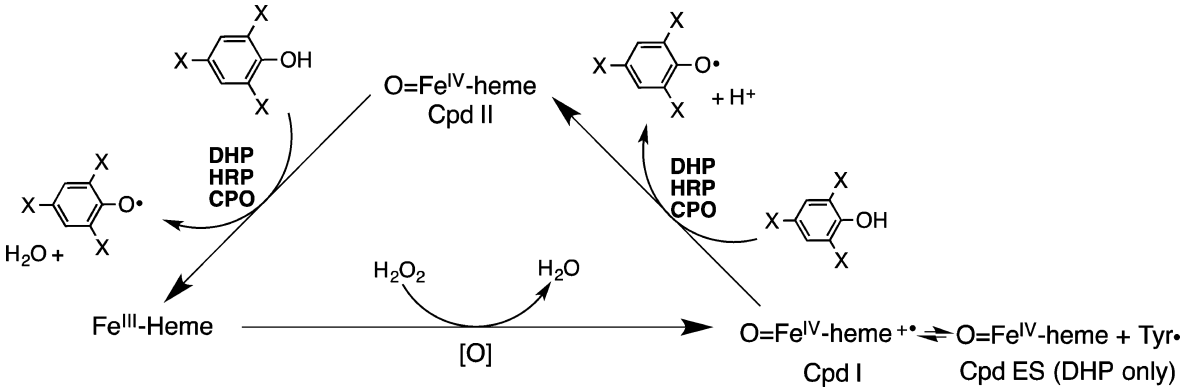


very similar structures while differing in only five amino acids.[1,23,24] This study will only focus on wild-type (WT) DHP A.

The major question of how DHP will interconvert the different oxidation states of the heme required by these two functions arises, i.e., the ferrous state for the $O_2$ carrier role vs the ferric state for the peroxidase activity. It has been shown that DHP can switch from the oxyferrous state to the ferric state via $H_2O_2$ oxidation, but this occurs only when substrate trihalophenol is present.[25,26] The triggering mechanism has been disputed by two research groups. Our lab has proposed a direct oxidation of the oxyferrous heme to the ferric state by substrate TCP radicals (TCP$^{\bullet}$) that are initially generated via oxidation of TCP by the peroxidase reaction of $H_2O_2$ in the presence of trace amounts of ferric DHP that exist in the oxyferrous protein sample.[25] Analogous results and mechanistic interpretations have been previously reported for the role of substrate radicals in the conversion of lignin peroxidase compound III (the nonphysiological oxyferrous state) to the active ferric enzyme.[27,28] On the other hand, Ghiladi and co-workers subsequently proposed that conversion of the ferrous state to the catalytically active species Cpd II is initiated by $H_2O_2$ replacing the bound $O_2$ upon substrate binding.[26] The latter mechanism is built on the experimental observation that Cpd II can be formed directly from deoxyferrous DHP by reaction with $H_2O_2$ alone.[26] However, such a reaction has only been demonstrated under anaerobic conditions. With $O_2$ bound to the ferrous heme, Cpd II DHP can not be formed upon addition of $H_2O_2$.[25,26] The lack of reactivity of oxyferrous DHP toward $H_2O_2$ in the absence of TXP may be physiologically significant because DHP primarily functions as an oxygen transport protein. The hypothesis of Ghiladi and co-workers that TCP binding triggers the formation of Cpd II by promoting the replacement of bound $O_2$ with $H_2O_2$ has been challenged by our recent $O_2$ affinity ($K_{O_2}$) study of DHP in which we reported that the $K_{O_2}$ value of DHP is barely affected by the presence of TCP.[3]

To clarify the unsettled functional switching mechanism of DHP, i.e., the $H_2O_2$-mediated oxidation of oxyferrous to ferric DHP, we have further probed the role of TCP in activating the peroxidase function from the $O_2$-carrying ferrous state of DHP. We have found that not only the substrate TCP and inhibitor/substrate 4-BP but also a structurally totally unrelated redox compound ferrocyanide, a known peroxidase substrate,[29] can trigger the functional switch. Furthermore, we have demonstrated that, when $[H_2O_2]$ <50 $\mu$M, the ferric heme ligands imidazole (Im) and cyanide ($CN^-$) as well as a spin-trapping reagent 5,5-dimethyl-1-pyrroline-*N*-oxide (DMPO) each alone can completely inhibit the TCP-triggered conversion of oxyferrous to ferric DHP. These and additional results on the $O_2$ concentration dependence of the conversion rates, shown in this study, are consistent with a conversion of oxy-DHP to the ferric state through direct oxidation of deoxyferrous DHP by TCP radicals as the initial step in the activation of oxy-DHP for peroxidase function.

## MATERIALS AND METHODS

**Materials.** Reagent-grade chemicals (Aldrich, ACROS, Cayman, or Fisher) were used without further purification. HRP (type VI, Rz 2.7) was purchased from Sigma-Aldrich. Wild-type six-His-tagged DHP was expressed and purified as previously described.[30] Protein concentrations were determined by the pyridine hemochromogen method ($\varepsilon_{555}$ = 34.4 $M^{-1}$ $cm^{-1}$)[31] and are the concentrations of the heme component. Homogeneous oxyferrous DHP was generated by addition of a slight excess of sodium dithionite to isolated DHP followed by Biogel P6DG (Bio-Rad) desalting column chromatography with 0.1 M potassium phosphate buffer (pH 7) at 4 °C.[25]

All stock solutions of chemicals were freshly made before experiments. The concentration of $H_2O_2$ diluted from a 30% stock solution was confirmed spectrophotometrically ($\varepsilon_{240}$ = 39.4 $M^{-1}$ $cm^{-1}$).[32] TCP and 4-BP stocks (10 mM) were made in a 50/50 (v/v) ethanol/deionized water mixture.

**Stopped-Flow Rapid Scan UV−Visible Spectrophotometric Studies.** Transient reactions and the detection of enzyme intermediates were performed on a stopped-flow spectrophotometer (1.0 cm path length, model SF-61 DX2 from Hi-Tech Scientific, Salisbury, U.K.) at 4 °C in 100 mM potassium phosphate buffer (pH 7.0) in the single-mixing mode. The double-mixing mode has also been used only for generation of Cpd ES DHP and its reaction with substrates. Fe(III) DHP is first mixed with 1.2 equiv of $H_2O_2$ allowing for Cpd ES to be fully formed (aging time of 15 s) and then mixed with substrates. Oxyferrous DHP at a final concentration of 5 $\mu$M (1 equiv) alone or containing TCP, 4-BP, or ferrocyanide was mixed with 0−40 equiv of $H_2O_2$. $H_2O_2$ solutions were prepared in $N_2$-saturated, air-equilibrated, and $O_2$-saturated potassium phosphate buffers and mixed with air-equilibrated buffer (containing oxy-DHP with or without TCP and with or without ferrocyanide) in the stopped-flow rapid scan apparatus (final $O_2$ concentrations of 0.20, 0.40, and 1.16 mM,


dx.doi.org/10.1021/bi5002757 | *Biochemistry* 2014, 53, 4956−4969

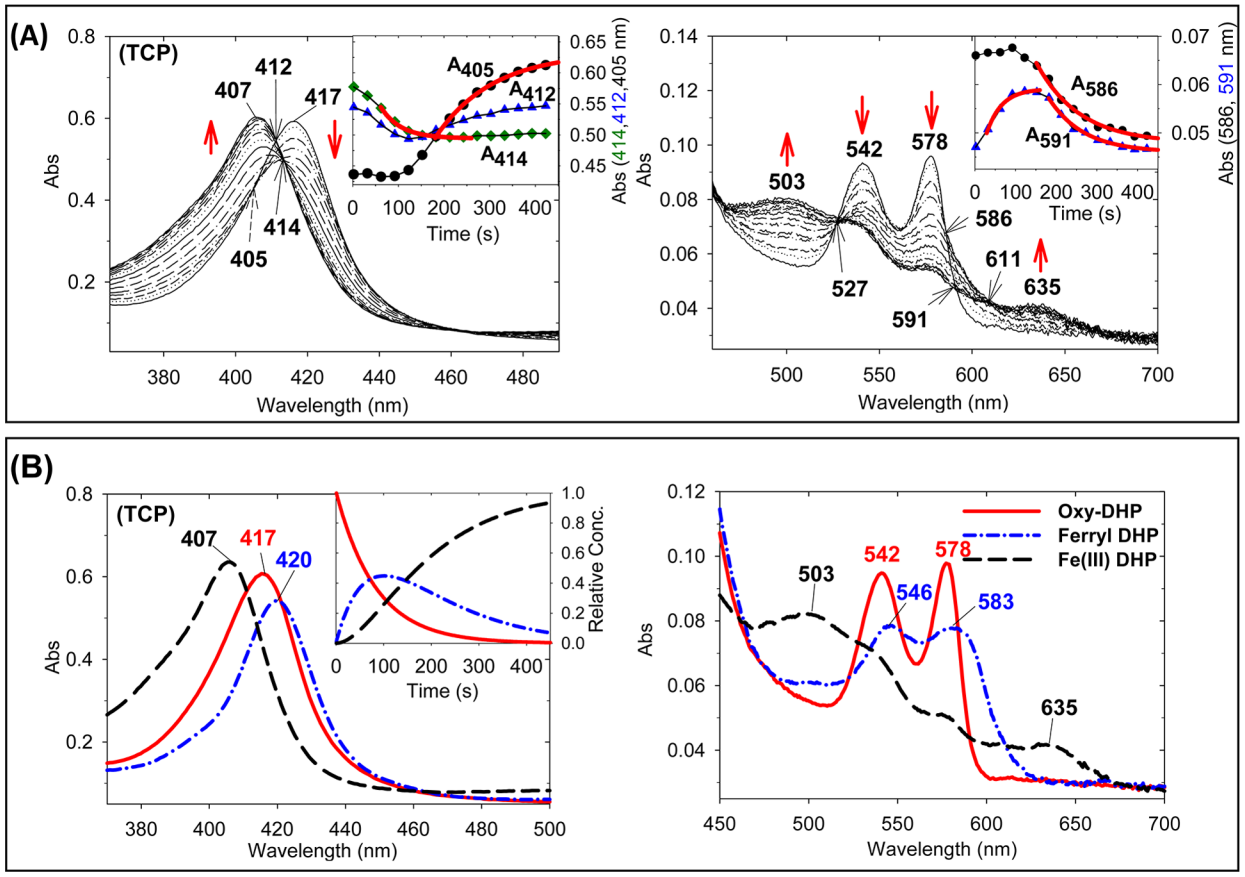


**Figure 1.** (A) Spectral change upon addition of 5 $\mu$M $H_2O_2$ to 5 $\mu$M oxyferrous DHP in the presence of 5 $\mu$M TCP. The insets in panel A show time-dependent absorbance changes at particular isosbestic points indicated to monitor the disappearance of oxy-DHP (green diamonds), the appearance of ferric DHP (black circles), and rise and decays of ferryl (Cpd ES) DHP (blue triangles). The red bold lines on the traces show exponential fits for the indicated time ranges and calculated apparent first-order rate constants. (B) UV−visible spectra of oxyferrous (red solid line), ferryl (dark green solid line), and ferric (blue dashed line) DHP obtained from global analysis of the data in panel A. The inset in panel B shows the relative concentration profile determined by global analysis.

respectively; 1.91 mM $O_2$ in the $O_2$-saturated solution at 4 °C).[33] $N_2$- and $O_2$-saturated buffers were prepared by continuously bubbling the buffers with a slow stream of these gases in rubber septum-sealed containers (with an outlet syringe needle) for >3 h on ice and transferred into a sample mounting chamber compartment of the stopped-flow rapid scan apparatus using a gastight syringe. Global analysis was performed using Specfit Global Analysis and fit to exponential functions as a two-step, three-species irreversible mechanism.

**Benchtop Mixing Kinetic Assays.** The inhibition reactions were monitored using a Cary 400 UV−visible spectrophotometer in a 1.0 cm path length cuvette at 4 °C. The oxy-DHP concentration in each sample was 5 $\mu$M in 100 mM potassium phosphate buffer (pH 7.0). The peroxidase substrates (TCP, 4-BP, or potassium ferrocyanide) and inhibitors (Im or $CN^-$) were first mixed with oxy-DHP in phosphate buffer (total volume of 0.7 mL) and incubated for 3 min in the cuvette. Subsequently, the $H_2O_2$ solution (a few microliters) was added to the cuvette to initiate the reaction.

**Gas Chromatography−Mass Spectrometry (GC−MS) Analyses.** An HP-5890 Restek RTX-5 GC capillary column (30 m × 0.32 mm) was used for detection of the products extracted from the aqueous solution by ethyl acetate. The initial temperature of the column was set at 50 °C for 2 min, and the temperature was subsequently increased at a rate of 10 °C/min to a final temperature of 300 °C and then held for 10 min. MS detection was in the electron impact (EI) ionization mode, and a VG70S mass spectrometer scanning from 50 to 450 amu was used for product identification.

## RESULTS

**TCP/$H_2O_2$-Triggered Conversion of Oxy-DHP to the Ferric State with 1 equiv of $H_2O_2$.** In our previous study, we demonstrated that conversion of oxy-DHP (5 $\mu$M) to the ferric enzyme requires the copresence of the substrates TCP and $H_2O_2$ using excess TCP (150 $\mu$M, 30 equiv) and 1 or 0.5 equiv of $H_2O_2$.[25] During the conversion, an absorption spectral change with a single set of isosbestic points (412, 528, and 592 nm) was observed, suggesting that no detectable intermediates are involved. To further probe the conversion mechanism, we have performed more detailed investigations of this study with an oxy-DHP:$H_2O_2$:substrate concentration ratio of 1:1:1. Figure 1A shows that in the presence of 1 equiv of TCP, 1 equiv of $H_2O_2$ readily converts oxy-DHP [417 (Soret), 542, and 578 nm] to the ferric state [407 (Soret), 503, and 635 nm] within a reaction time of 450 s. Under these conditions, the spectral changes exhibit three sets of isosbestic points, indicating that another enzyme species is involved as an intermediate during the conversion.

The three sets of isosbestic point in Figure 1A are nearly identical to those for oxy-DHP/Cpd ES (394 and 586 nm), Cpd ES/ferric (414 and 611 nm), and oxy-DHP/ferric DHP


dx.doi.org/10.1021/bi5002757 | Biochemistry 2014, 53, 4956−4969

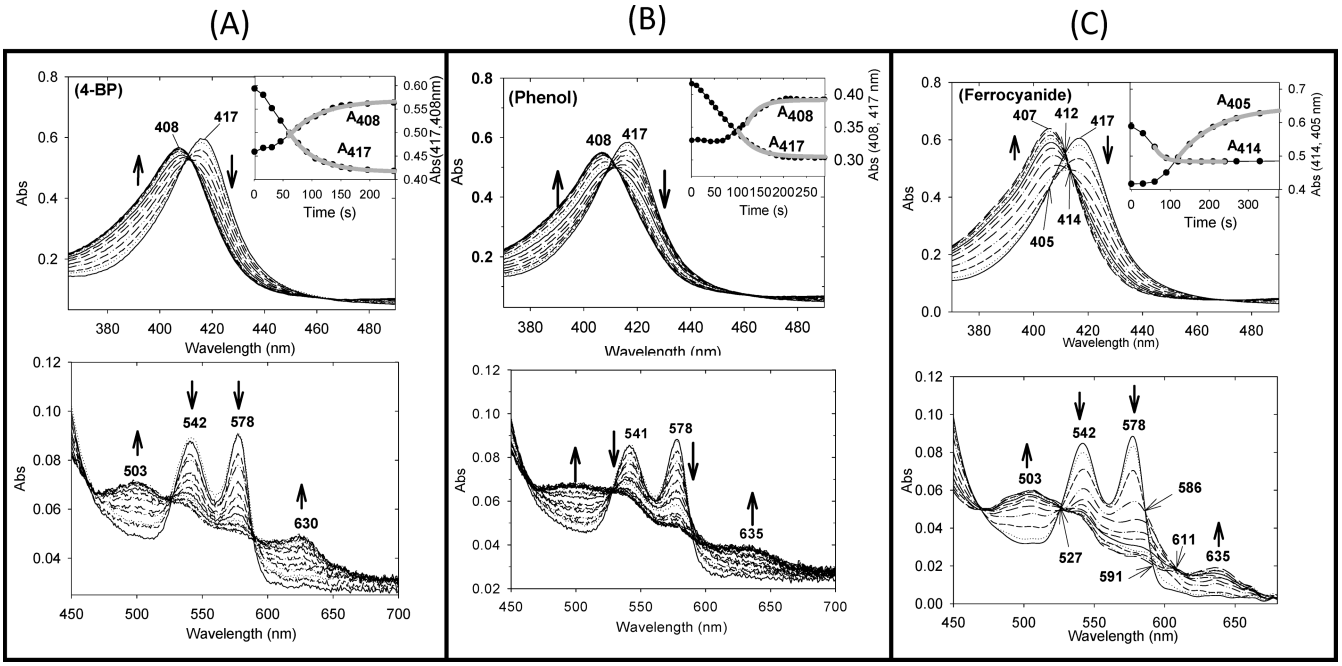


**Figure 2.** Spectral change upon addition of 5 $\mu$M $H_2O_2$ to 5 $\mu$M oxyferrous DHP in the presence of (A) 150 $\mu$M 4-BP, (B) 150 $\mu$M phenol, and (C) 5 $\mu$M potassium ferrocyanide. The insets in the top panels show the time-dependent absorbance changes at selected isosbestic points to monitor the disappearance of oxy-DHP [417 nm (A and B) and 414 nm (C)] or the appearance of ferric DHP [408 nm (A and B) and 405 nm (C)]. The bold lines on the traces show exponential fits for the indicated time ranges. Apparent first-order rate constants ($k_{obs}$) obtained from the fits are $2.3 \times 10^{-2}$ $s^{-1}$ ($A_{417}$) and $1.9 \times 10^{-2}$ $s^{-1}$ ($A_{408}$) in panel A, $2.9 \times 10^{-2}$ $s^{-1}$ ($A_{417}$) and $3.0 \times 10^{-2}$ $s^{-1}$ ($A_{408}$) in panel B, and $4.8 \times 10^{-2}$ $s^{-1}$ ($A_{414}$) and $1.0 \times 10^{-2}$ $s^{-1}$ ($A_{405}$) in panel C.

(412 and 591 nm) based on overlaid normalized absorption spectra of these three DHP species (Figure S1A of the Supporting Information), indicating that ferryl DHP is formed as an intermediate in the reaction. The difference between the isosbestic point seen at 394 nm for oxy-DHP/Cpd ES in Figure S1A of the Supporting Information and the actual isosbestic point at 404 nm in the time-dependent spectral changes (Figure 1A) can be explained by simulated spectral changes for the three DHP forms (Figure S1B of the Supporting Information) that yield a shifted (from 394 to 404 nm) position for this particular isosbestic point. This shift is probably observed because of the less than stoichiometric formation of ferryl DHP. The formation of the ferryl intermediate is also supported by the global analysis result for the reaction described above as shown in Figure 1B [absorption peaks at 420 (Soret), 545, and 583 nm, dark green dotted–dashed line], whose maximal amount reaches only ~45% of the total DHP concentration.

On the basis of the assignment described above, the time-dependent absorption changes at two observed Soret isosbestic points (at 414 nm for Cpd ES/ferric DHP and 405 nm for oxy-DHP/Cpd ES) could represent the time-dependent disappearance of oxy-DHP (dark green diamond) and the appearance of ferric species (black circles), respectively, as shown in the inset of the left panel of Figure 1A. These spectral changes are coupled with the rise (absorption decrease) and decay (absorption increase) of the ferryl intermediate as indicated by the absorption changes at 412 nm, an isosbestic point for oxy-DHP/ferric DHP as a function of time (blue triangles in Figure 1A, inset of the left panel). A similar result in the visible region at 591 nm was also observed for the appearance (first phase) and disappearance (second phase) of the ferryl intermediate (blue triangles) as well as at 586 nm for the rise (absorption decrease) of ferric DHP (Figure 1A, inset of the right panel, black circles). We have calculated the apparent rate constant ($k_{obs}$) from the exponential part (bold red lines) of these absorption changes for the disappearance of oxy-DHP [$(2.3 \pm 0.1) \times 10^{-2}$ $s^{-1}$ ($A_{414}$)], the appearance of ferric DHP [$(8.4 \pm 0.1) \times 10^{-3}$ $s^{-1}$ ($A_{405}$) and $(9.4 \pm 0.2) \times 10^{-3}$ $s^{-1}$ ($A_{586}$), which are considered practically identical], the appearance of ferryl DHP [$(2.7 \pm 0.1) \times 10^{-2}$ $s^{-1}$ ($A_{591}$)], and the disappearance of ferryl DHP [$(1.2 \pm 0.1) \times 10^{-2}$ $s^{-1}$ at ($A_{591}$)]. Even though these $k_{obs}$ values were obtained under the non-pseudo-first-order reaction conditions, the reaction traces nicely fit exponential decays or emergences of the three species, and thus, these values can provide a convenient way to estimate the true second-order rate constants ($k$) based on the equation $k_{obs} \sim k[TCP]_o$ or $k_{obs} \sim k[H_2O_2]_o$, where $[TCP]_o$ and $[H_2O_2]_o$ are the initial concentrations of TCP and $H_2O_2$, respectively.[34] The $k_{obs}$ values thus obtained may be useful in evaluating the relative rates among different reactions to interpret the reaction mechanisms as done in this study. Note that the rise of the ferryl DHP species starts slowly with an apparent lag time period before its formation rate reaches a maximum (see Figure 1A insets, blue triangles), suggesting that there is yet another species being formed prior to the formation of ferryl DHP (*vide infra*).

**$H_2O_2$-Mediated Conversion of Oxy-DHP to Ferric DHP Triggered by 4-BP or Ferrocyanide/Ferricyanide.** Reactions of oxy-DHP with $H_2O_2$ in the presence of 4-BP are shown in Figure 2A. The maximal activation rate in the presence of excess 4-BP (150 $\mu$M) is $(2.3 \pm 0.1) \times 10^{-2}$ $s^{-1}$, which is as fast as the conversion triggered by 1 equiv of TCP [$(2.3 \pm 0.1) \times 10^{-2}$ $s^{-1}$ (Figure 1A)]. In the presence of only 1 equiv of 4-BP, the rate is considerably slower [$(6.9 \pm 0.5) \times 10^{-3}$ $s^{-1}$ (not shown)] than that with TCP by ~3.4-fold. Underivatized


dx.doi.org/10.1021/bi5002757 | *Biochemistry* 2014, 53, 4956–4969

phenol is also able to induce the $H_2O_2$ oxidation of oxy-DHP at a comparable rate [$(3.1 \pm 0.1) \times 10^{-2}$ $s^{-1}$, at 150 $\mu$M (Figure 2B)].

Surprisingly, ferrocyanide, a known peroxidase substrate[29] with a structure that is totally different from those of DHP substrates, can also trigger the functional switch of oxy-DHP. Figure 2C shows that in the presence of 1 equiv of ferrocyanide, oxy-DHP quickly switches to the ferric state upon reaction with 1 equiv of $H_2O_2$. The spectral change for the ferrocyanide-triggered conversion of oxy-DHP is not significantly different from that for the TCP-triggered one, except that the rate is about 2 times greater [$(4.8 \pm 0.2) \times 10^{-2}$ $s^{-1}$ vs $(2.3 \pm 0.1) \times 10^{-2}$ $s^{-1}$] under the same conditions. A similar conversion has also been seen in the presence of another structurally unrelated compound, potassium iodide (KI), but only at acidic pH (data not shown). In fact, iodide is known to be a reductant (substrate) for HRP Cpd I preferably at acidic pH values.[12] The apparent conversion rates, $k_{obs}$ ($k_{414}$ for TCP) values, of oxy-DHP triggered by TCP and other various substrates (4-BP, phenol, and ferrocyanide) for DHP are listed in Table 1.

**Table 1. Apparent First-Order Reaction Rate Constants ($k_{obs}$) for the Conversion of Oxy-DHP to Ferric DHP Triggered by Various Peroxidase Substrates at pH 7.0 and 4 °C[a]**

| substrate | $k_{obs}$ ($s^{-1}$) |
|---|---|
| TCP | $(2.3 \pm 0.1) \times 10^{-2}$ |
| 4-BP | $(6.9 \pm 0.5) \times 10^{-3}$ |
| phenol | $(3.1 \pm 0.1) \times 10^{-2}$ |
| ferrocyanide | $(4.8 \pm 0.2) \times 10^{-2}$ |

[a]All rates are determined by analyzing the time-dependent absorbance changes at 414 nm (TCP and ferrocyanide) or 417 nm (4-BP and phenol) for the disappearance of oxy-DHP. Concentrations of oxy-DHP, $H_2O_2$, and substrates are all 5 $\mu$M except that of phenol, which is 150 $\mu$M.

TCP and ferrocyanide presumably trigger the switch of oxy-DHP to the ferric state by serving as peroxidase substrates for the trace amount of ferric DHP in the oxy-DHP sample in the presence of $H_2O_2$. This would then generate TCP radical (TCP$^\bullet$) and ferricyanide, respectively, which, in turn, would serve as an oxidant to convert oxy-DHP to the ferric state. Thus, ferricyanide would serve the same role as TCP$^\bullet$ in the switching mechanism. To directly test this hypothesis, we have monitored the spectral change for the reaction of oxy-DHP with 1.0 equiv of ferricyanide (in place of ferrocyanide) and 1.0 equiv of $H_2O_2$ as shown in Figure 3. Similar to the cases with TCP (Figure 1A) and ferrocyanide (Figure 2C), three sets of isosbestic points are observed as shown in Figure 3A and assigned to those for oxy-DHP/Cpd ES (586 nm), Cpd ES/ferric (414 and 611 nm), and oxy-DHP/ferric DHP (412 and 591 nm). Thus, the change of oxy-DHP, ferryl DHP, and ferric DHP species can be represented by the time course traces for 611, 591, and 586 nm, respectively, as shown in Figure 3B. Different from the conversion reaction with ferrocyanide, the reaction with ferricyanide (blue triangles) consists of a fast phase [0–25 s (enlarged in the bottom panel of Figure 3B)], followed by a slow phase [75–300 s (Figure 3B, top)]. In the fast phase (Figure 4B, bottom), ferric DHP is formed before formation of ferryl DHP as indicated by the decrease in $A_{586}$ to the nearly constant value (blue triangles) versus the small change in $A_{591}$ (black circles for ferryl DHP) for the first ~5 s. After the ferric species stops accumulating, ferryl DHP starts to arise until it reaches its maximal amount at the end of the fast phase (~25 s). At a later stage (75–300 s), ferryl DHP decays (black circles) in a manner concomitant with further formation of ferric DHP (blue triangles) at a rate of ~0.008 $s^{-1}$. The bimolecular rate constants for the step of ferricyanide oxidizing oxy-DHP to the ferric state as well as for other steps involved in the reaction described above have been separately determined using a stopped-flow technique in this study (see Discussion).

**Effects of >1 equiv (2.5–40 equiv) of $H_2O_2$ on the TCP/$H_2O_2$-Triggered and Ferrocyanide/$H_2O_2$-Triggered Conversion of Oxy-DHP to the Ferryl State.** The conversion reaction rates with higher $H_2O_2$ concentrations of up to 200 $\mu$M (40 equiv) in the presence of 1 equiv of TCP or ferrocyanide were also measured (Table 2). Only 1 equiv (5 $\mu$M) of TCP or ferrocyanide was used with 2.5–40 equiv of $H_2O_2$ in this study to prevent multiple cycles of reaction(s) from occurring. Note that, in the presence of 1 equiv of TCP, the end product of the reaction of oxy-DHP with 1 equiv of $H_2O_2$ is ferric DHP, while reactions with >1 equiv of $H_2O_2$ (2.5–40 equiv) result in the formation of ferryl (Cpd II or Cpd ES) DHP in the first phase as demonstrated in Figure 4A (black overlaid spectra). This is followed by slower conversion to another species that may be characterized as Cpd RH, a nonproductive enzyme form in the second phase (green overlaid spectra). Cpd RH is usually relatively slowly formed following the reactions of ferric or oxy-DHP with excess amounts of $H_2O_2$ in the absence of substrate (e.g., TCP).[4,35] We noticed that an increase in the amount of $H_2O_2$ from 1 to ≥5 equiv under these conditions only slightly increases the conversion rates (~1.13-fold). However, the conversion rate does not significantly increase further when the amount of $H_2O_2$ is increased from 5 to 10, 20, and 40 equiv. Parallel experiments in the presence of 1 equiv of ferrocyanide in place of TCP resulted in a similar outcome except that increases in the conversion rates with >5 equiv of $H_2O_2$ are 2.2–2.7-fold faster (Table 2, far right column) compared with rates 1.1–1.3-fold faster observed with TCP, yet the conversion rate was not dependent on the $H_2O_2$ concentration at 10–40 equiv as is the case for TCP.

**Effects of $O_2$ Concentration on the TCP/$H_2O_2$-Triggered and Ferrocyanide/$H_2O_2$-Triggered Conversion of Oxy-DHP to the Ferric or Ferryl State in the Presence of 1 or 20 equiv of $H_2O_2$.** We have also examined the effects of $O_2$ concentration on the conversion rates at three varying $O_2$ concentrations of 0.20, 0.40, and 1.16 mM (see Materials and Methods). Results shown in Table 3 indicate that the conversion rates become detectably faster by 20–25% when the $O_2$ concentration is decreased to approximately half for all four cases (1 equiv of TCP or ferrocyanide with 1 and 20 equiv of $H_2O_2$), while increasing the $O_2$ concentration from 0.40 to 1.16 mM noticeably decreases the reaction rates (to ~60 and ~45% with 1 and 20 equiv of $H_2O_2$, respectively, for TCP; corresponding values for ferrocyanide were ~47 and ~23%, respectively). Thus, even though the magnitudes of the effects of the higher $O_2$ concentration are somewhat greater with ferrocyanide than with TCP, both demonstrate very similar trends in terms of the $O_2$ concentration dependence of the conversion rates.

**Inhibitory Effects of Ferric Heme Protein Ligands and the Spin Trap Reagent DMPO on the Functional Switching of Oxy-DHP.** In our previously proposed functional switching mechanism for DHP, we speculated that the


dx.doi.org/10.1021/bi5002757 | Biochemistry 2014, 53, 4956–4969

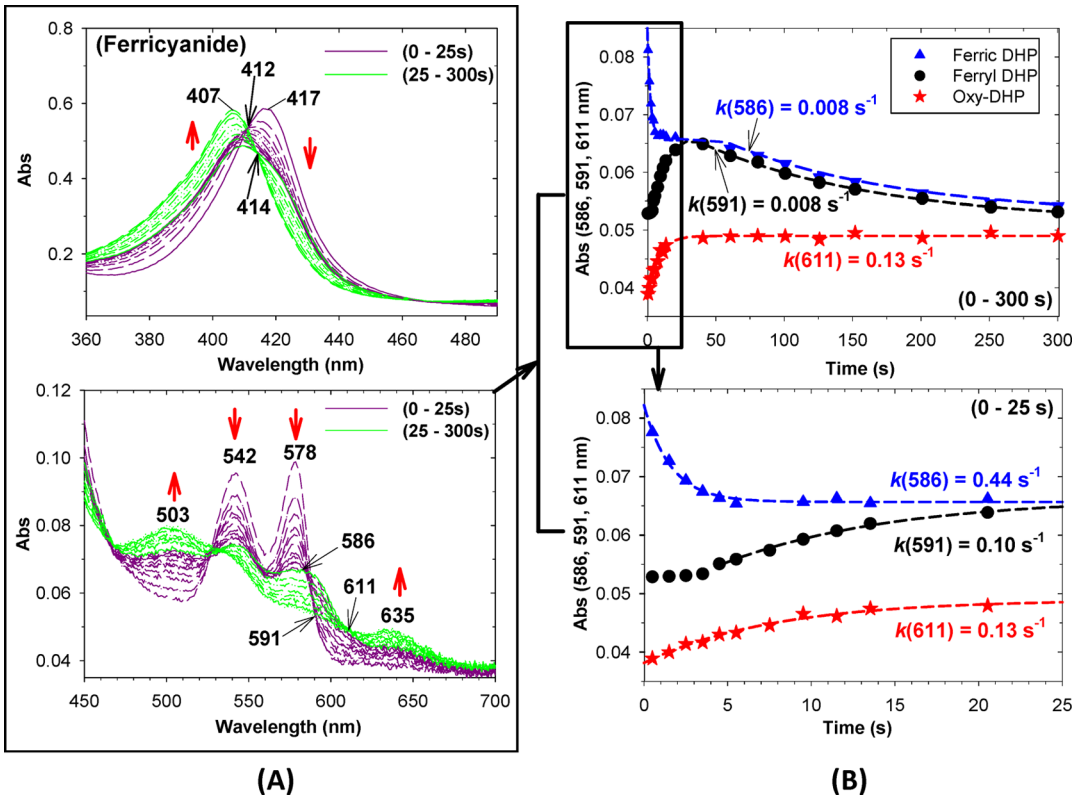


**Figure 3.** (A) Spectral changes upon addition of a mixed solution of 5 $\mu$M $H_2O_2$ and 5 $\mu$M potassium ferricyanide to 5 $\mu$M oxyferrous DHP for time periods of 0−25 s (dark pink) and 25−300 s (green). (B) Time-dependent absorbance changes at particular isosbestic points in panel A for monitoring the disappearance of oxy-DHP ($A_{611}$, red stars), the appearance of ferric DHP ($A_{586}$, blue triangles), and the rise and decays of ferryl ($A_{591}$, Cpd ES) DHP (black circles). The isosbestic point at 586 nm is observed near the end of the first phase (dark pink lines) and at the beginning of the second phase (green lines) following the appearance of an initial isosbestic point (~591 nm). The dashed lines on the plots show exponential fits for the indicated time ranges and calculated apparent first-order rate constants.

peroxidase activity of a trace amount of Fe(III) enzyme is critical in initiating the conversion by generating $TCP^{\bullet}$ as an oxy-DHP oxidant. To further test this proposed mechanism, reagents that bind to and thereby inhibit the activity of the ferric enzyme or that trap the TCP radicals were added to the oxy-DHP to ferric DHP conversion reaction mixture. Cyanide (KCN) and imidazole (Im) are both ferric heme ligands [$K_d$ values for their complexes with ferric DHP at pH 7.0 and 4 °C were ~0.5 $\mu$M for cyanide and ~0.2 mM for Im (this study)], and they have much weaker affinities for the ferrous heme proteins [e.g., $K_d$ values of $10^{-1}$ to 1 M (cyanide)[36] and $10^{-1}$ to 10 M (Im)[37] for deoxyferrous Mb at pH 7.0]. As shown in Figure 5, both Im (20 mM, panel A) and KCN (5 mM, panel B) are able to totally inhibit the TCP-triggered conversion of oxy-DHP, as indicated by the absence of absorption changes at 417 nm (Soret peak) upon addition of 1 equiv of $H_2O_2$ and 1 equiv of TCP to oxy-DHP (0−600 s). Inhibition by $CN^-$ or Im was also observed in the ferrocyanide-triggered conversion of oxy-DHP (Figure 6). In addition, inhibition by Im can be reversed by adding a small amount of HRP (0.5%, 25 nM), which generates TCP radicals by catalyzing the TCP oxidation by $H_2O_2$.[13,14] As shown in Figure 5A (600−800 s), addition of HRP results in the transformation of oxy-DHP [417 (Soret), 542, and 578 nm] to the Fe(III)-Im DHP complex [415 (Soret) and 538 nm] ($k_{obs}$ = 0.009 $s^{-1}$). On the other hand, addition of HRP (0.5%, 25 nM at 600 s) to the $CN^-$-inhibited oxy-DHP to ferric DHP conversion mixture had little effect (Figure 5B). This is due to the fact that ferric HRP has a very low affinity for Im [negligible binding at 20 mM (this study)] but has a high affinity for cyanide (tight binding with a $K_d$ of 2.5−3.0 × $10^{-6}$ M at pH 7[38]), and thus, the peroxidase activity of HRP was completely inhibited in the presence of $CN^-$ (5 mM).

Next, to directly prove the involvement of TCP radicals in the functional switch of oxy-DHP, the spin-trapping reagent DMPO (see Figure S2 of the Supporting Information for its structure) that potentially traps TCP radicals was introduced to the switching process. A complete inhibition of the 5 $\mu$M TCP- or 4-BP-triggered conversion of oxy-DHP to ferric DHP by 10 mM DMPO was observed as shown in panel A or B of Figure 7, respectively. Such inhibition with 5 $\mu$M TCP was also observed with the amount of $H_2O_2$ increased to 5 (25 $\mu$M) and 10 equiv (50 $\mu$M), but more DMPO (50 and 100 mM, respectively) was needed to achieve complete or nearly complete inhibition (plots not shown). When the $H_2O_2$ concentration was further increased to 100 $\mu$M, complete inhibition of the first phase was not achieved even with 100 mM DMPO [~65% inhibition in terms of conversion rate (Figure 4B)]. However, it appears that the second phase of the spectral changes was effectively inhibited by 100 mM DMPO. Im (100 mM) was able to inhibit only ~80% of the reaction, exhibiting a single-phase spectral change to the ferric-Im complex (spectra not shown). Addition of 5 mM cyanide totally prevented the spectral change of oxy-DHP even with 40 equiv (0.2 mM) of $H_2O_2$ (spectra not shown). Significantly, DMPO (10 mM) has no effect on the ferrocyanide-triggered conversion of oxy-DHP to ferric DHP [$k_{obs}$ values of (4.7 ± 0.1) × $10^{-2}$ $s^{-1}$ (Figure 7C) and (4.8 ± 0.2) × $10^{-2}$ $s^{-1}$ (with 5 $\mu$M ferrocyanide and 5 $\mu$M $H_2O_2$)


dx.doi.org/10.1021/bi5002757 | Biochemistry 2014, 53, 4956−4969

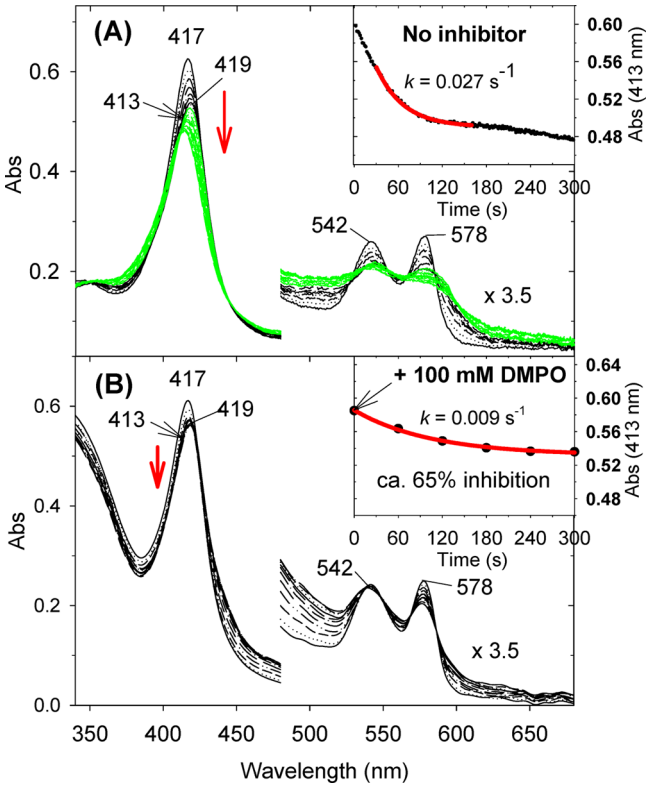


**Figure 4.** UV−visible spectroscopic monitoring upon mixing (concentrations after mixing) 100 $\mu$M $H_2O_2$ with 5 $\mu$M oxy-DHP containing 5 $\mu$M TCP in the absence (A) or presence (B) of 100 mM DMPO. The insets show the plots of absorbance at 413 nm as a function of time. Apparent first-order rate constants that are calculated from an exponential fit (red bold solid line) are indicated ($k \sim 0.027$ $s^{-1}$). In panel A, two phases of the spectral changes are colored black (first phase) and green (second phase). The absorbance change at 413 nm instead of 417 nm is monitored because $A_{417}$ vs time does not give a clear ending of the first phase in panel A (plot not shown). A similar $k$ value (~0.025 $s^{-1}$) can be obtained from the plot of $A_{417}$ vs time (0−300 s) for the first phase when all the data points are fit to double-phase exponential decays (not shown).

**Table 2. Effects of $H_2O_2$ Concentrations (5−40 equiv of 5 $\mu$M oxy-DHP) on the Conversion Rates (measured on the basis of the absorbance change at 413.7 nm, one of the instrument-set wavelength points for absorbance recording) from Oxy-DHP to Ferryl [Fe(IV)] DHP in the Presence of 1 equiv of TCP or Ferrocyanide[a]**

| $H_2O_2$ (equiv) (1 equiv = 5 $\mu$M) | $k_{413.7}$ ($s^{-1}$) with TCP (5 $\mu$M) | $k_{413.7}$ ($s^{-1}$) with ferrocyanide (5 $\mu$M) |
|---|---|---|
| 1[b] | 100%[c] | 100%[d] |
| 2.5 | (105 ± 16)% | (171 ± 16)% |
| 5 | (113 ± 9)% | (219 ± 15)% |
| 10 | (113 ± 6)% | (271 ± 11)% |
| 20 | (113 ± 9)% | (272 ± 8)% |
| 40 | (127 ± 10)% | (272 ± 18)% |

[a]The measurements were performed in 0.1 M potassium phosphate buffer (pH 7.0) at 4 °C. See the text for additional information. [b]Conversion to ferric DHP. [c]Rate of (0.019 ± 0.003) $s^{-1}$. [d]Rate of (0.041 ± 0.007) $s^{-1}$.

**Table 3. Effects of $O_2$ Concentrations (0.20, 0.40, and 1.16 mM) on the Conversion Rate (measured on the basis of the absorbance change at 413.7 nm) from Oxy-DHP to Ferric DHP (with 1 equiv of $H_2O_2$) or to Ferryl [Fe(IV)] DHP (with 20 equiv of $H_2O_2$) in the Presence of 1 equiv of TCP or Ferrocyanide[a]**

| $[O_2]$ (mM) | $k_{413.7}$ ($s^{-1}$)[b] with TCP (5 $\mu$M): 1 equiv of $H_2O_2$ | with TCP (5 $\mu$M): 20 equiv of $H_2O_2$ | with ferrocyanide (5 $\mu$M): 1 equiv of $H_2O_2$ | with ferrocyanide (5 $\mu$M): 20 equiv of $H_2O_2$ |
|---|---|---|---|---|
| 0.20 | (117 ± 3)% | (123 ± 6)% | (118 ± 5)% | (128 ± 4)% |
| 0.40 | 100%[c] | 100%[d] | 100%[e] | 100%[f] |
| 1.16 | (61 ± 5)% | (45 ± 3)% | (47 ± 2)% | (23 ± 2)% |

[a]The measurements were performed in 0.1 M potassium phosphate buffer (pH 7.0) at 4 °C. See Materials and Methods for technical details. [b]Values are expressed in percent vs the mean values for air-saturated (0.40 mM $O_2$) oxy-DHP solution samples. [c]Rate of (0.019 ± 0.003) $s^{-1}$. [d]Rate of (0.027 ± 0.004) $s^{-1}$. [e]Rate of (0.041 ± 0.007) $s^{-1}$. [f]Rate of (0.105 ± 0.028) $s^{-1}$.

(Figure 3C)], indicating that the DMPO inhibition on the functional switch can occur only through trapping of the halophenolic radicals.

Attempts to detect and identify the trapped product (DMPO-TCP radical) by GC−MS were not successful, probably because of the likely low stability of this adduct. However, we have been able to detect a DMPO adduct of 4-BP ($m/z$ 285) formed in the DHP-catalyzed $H_2O_2$ oxidation of 4-BP in the presence of DMPO (Figure S2 of the Supporting Information).

**Determination of $O_2$ Dissociation Rate Constants [$k_{d(O_2)}$] of Oxy-DHP in the Absence and Presence of the Substrate TCP.** Although we have shown in our previous study that the substrate TCP (up to 2 mM) has very little effect on the $O_2$ affinity (equilibrium constant) of ferrous DHP,[3] we have not ruled out a possible influence of TCP on the $O_2$ binding kinetics of DHP that might be related to the roles of the substrate in triggering the functional conversion of the protein. In this study, $O_2$ dissociation rate constants [$k_{d(O_2)}$] were measured by a dithionite method (see Chapter 9 of ref 36) that involves rapidly mixing an anaerobic 40 mM dithionite solution with 10 $\mu$M oxy-DHP (concentrations before mixing) both in buffer [0.1 M potassium phosphate (pH 7.0)] at 4 °C (Figure S3 of the Supporting Information). The $k_{d(O_2)}$ values thus measured in the absence and presence of 1 mM TCP were 39.2 ± 1.2 and 37.6 ± 1.0 $s^{-1}$, respectively. The rate constants for TCP-free and TCP-bound oxy-DHP are essentially the same within experimental error. Using the previously determined $O_2$ dissociation equilibrium constants ($K_{O_2}$) under similar conditions,[3] $O_2$ association rate constants [$k_{a(O_2)}$] can be calculated with the equation $K_{O_2} = k_{d(O_2)}/k_{a(O_2)}$ as $k_{a(O_2)} = 39.2/(3.2 \times 10^{-6}) = 1.23 \times 10^7$ $M^{-1}$ $s^{-1}$ (without TCP) and $37.6/(3.5 \times 10^{-6}) = 1.10 \times 10^7$ $M^{-1}$ $s^{-1}$ (with 1 mM TCP). These $O_2$ association rate constants are comparable to the corresponding values for horse and sperm whale Mbs ($1.3 \times 10^7$ and $1.9 \times 10^7$ $M^{-1}$ $s^{-1}$, respectively, measured at 20 °C) (Chapter 9 of ref 35). Thus, TCP does not significantly affect the $O_2$ binding equilibrium or kinetic properties of ferrous DHP.


dx.doi.org/10.1021/bi5002757 | Biochemistry 2014, 53, 4956−4969

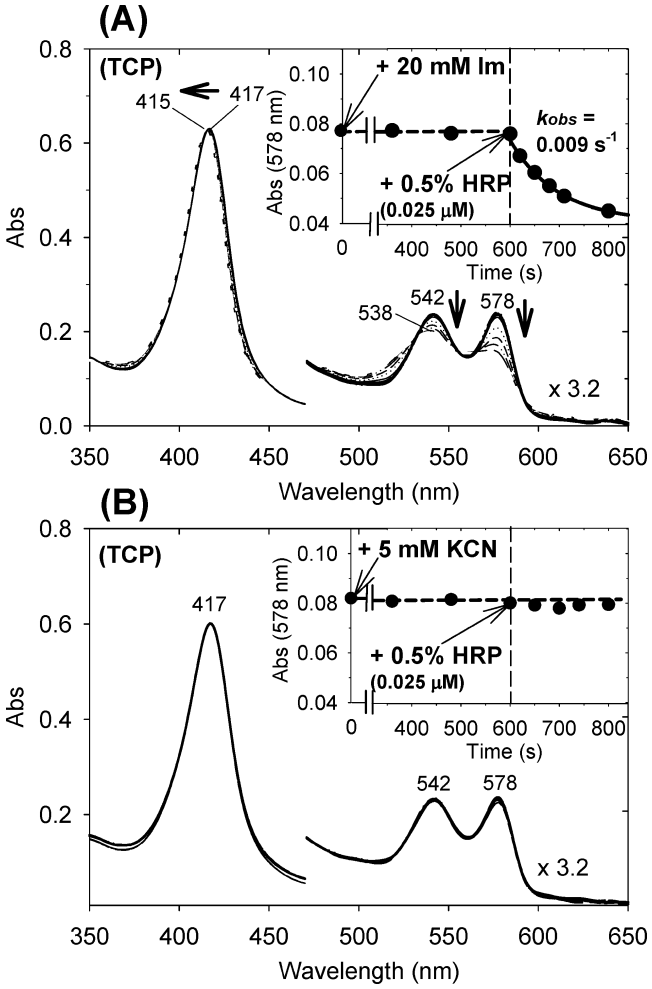


**Figure 5.** UV−visible spectroscopic monitoring upon addition of 5 $\mu$M $H_2O_2$ to a mixture of 5 $\mu$M oxy-DHP and (A) 20 mM Im or (B) 5 mM KCN in the presence of 5 $\mu$M TCP during a period of 0−600 s and upon subsequent addition of 25 nM (0.025 $\mu$M) HRP at 600 s (0.005 equiv, 0.5%) during a period of 600−800 s. The black circles in the insets show the plots of absorbance at 578 nm ($A_{578}$) as a function of time. The black dashed lines are drawn through the black circles, and the solid line (600−800 s in panel A) is the fit to an exponential decay curve that yields an apparent first-order rate constant ($k_{obs}$) of 0.009 $s^{-1}$.

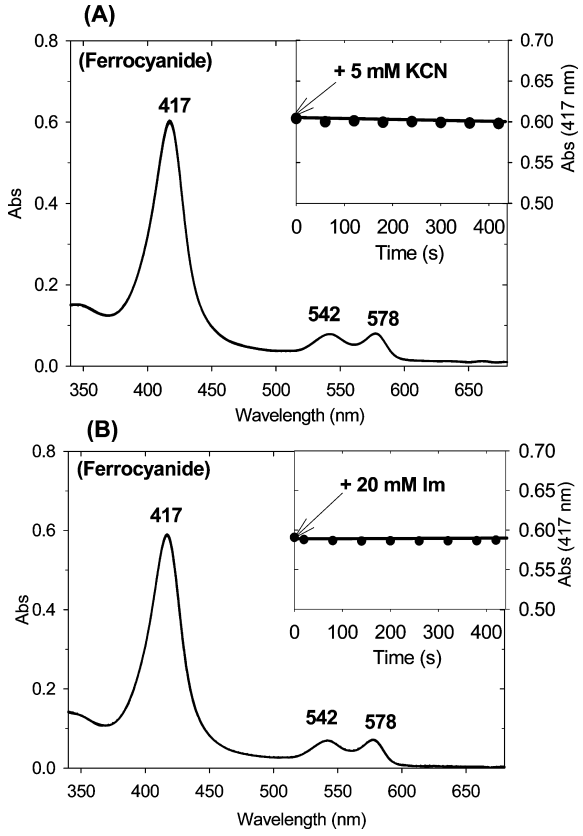


**Figure 6.** UV−visible spectroscopic monitoring upon addition of 5 $\mu$M $H_2O_2$ to the mixture of 5 $\mu$M oxy-DHP and (A) 5 mM KCN or (B) 20 mM Im in the presence of 5 $\mu$M potassium ferrocyanide (0−420 s). The insets show the plots of absorbance change at 417 nm as a function of time with a solid line drawn over the data points.

**Kinetics of Oxidation of Ferrous DHP by Ferricyanide.** To gain further information about the roles of ferricyanide and, by inference, TCP radical in the functional conversion of oxy-DHP to ferric DHP, we have also performed a kinetic study of the oxidation of oxy-DHP with a fixed concentration (1 mM) of ferricyanide at three different $O_2$ concentrations (0.20, 0.44, and 1.16 mM) using a stopped-flow rapid scan method. A plot of the reciprocal values of the observed rate constants ($k_{obs}$, $s^{-1}$) versus $O_2$ concentration can be reasonably well fit by a straight line with a slope of 0.202 s/mM (Figure 8, dotted line, for three filled circles) or 0.194 s/mM [Figure 8, solid line, for three filled circles and one timse sign (see below)]. This plot was made following the analysis of a similar reaction of oxy-Mb with ferricyanide by Antonini and collaborators.[39] According to their analysis, the *Y*-intercept should be equal to $1/k_{d(O_2)}$ (where $k_d$ is the $O_2$ dissociation rate constant from oxy-DHP or oxy-Mb). Also according to the theoretical analysis of the plot by the same authors[39] (see also Chapters 8 and 12 of ref 36), the slope of the linear correlation should be equal to $k_{a(O_2)}/[k_{d(O_2)}k_{ox(F)}[\text{ferricyanide}]]$, where $k_{ox(F)}$ is the rate constant ($M^{-1}$ $s^{-1}$) for the oxidation of deoxyferrous Mb (DHP) with ferricyanide [$k_{a(O_2)}$ and $k_{d(O_2)}$ are defined in the preceding section].

Because the $k_{d(O_2)}$ [39.2 $s^{-1}$ (Figure S3A of the Supporting Information)] and $k_{a(O_2)}$ values for oxy-DHP are now available (*vide supra*), the $k_{ox(F)}$ value can be calculated by using the slope of 0.194 s/mM in Figure 8, as 1.61 × $10^6$ $M^{-1}$ $s^{-1}$ for deoxyferrous DHP oxidation by ferricyanide under the conditions used [0.1 M potassium phosphate buffer (pH 7.0) at 4 °C]. This $k_{ox(F)}$ value is similar to the corresponding rate constants for deoxyferrous horse Mb {$k_{ox(F)}$ = [1.5 (12 °C) − 1.8 (19 °C)] × $10^6$ $M^{-1}$ $s^{-1}$}.[39]

## DISCUSSION

In this study, we have found that not only TCP but also 4-BP, phenol, ferrocyanide, and KI can trigger the $H_2O_2$-dependent conversion of oxy-DHP [apparent conversion rates ($k_{obs}$) listed in Table 1]. Because these five compounds have different structures (especially the first three phenol derivatives vs ferrocyanide and KI) yet are peroxidase substrates, i.e., electron donors, it is quite likely that substrate oxidation is involved in the conversion mechanism. In agreement with this supposition, we recently showed that addition of TCP or 4-BP (up to 2 mM; cf. $K_m$ ∼ 0.3 mM for TCP[40]) does not affect the $K_{O_2}$


dx.doi.org/10.1021/bi5002757 | *Biochemistry* 2014, 53, 4956−4969

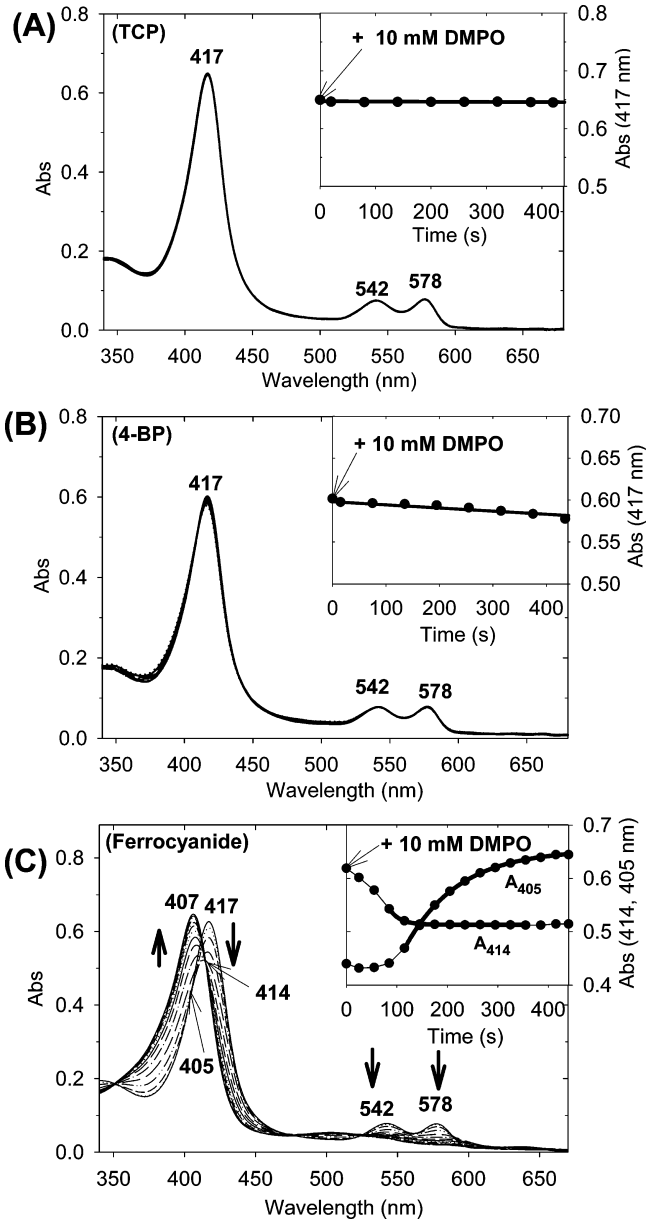


**Figure 7.** UV−visible spectroscopic monitoring upon addition of 5 $\mu$M $H_2O_2$ to the mixture of 5 $\mu$M oxy-DHP and 10 mM DMPO in the presence of (A) 5 $\mu$M TCP, (B) 150 $\mu$M 4-BP, or (C) 5 $\mu$M potassium ferrocyanide for a period of 0−420 s. The insets in panels A and B show plots of absorbance at 417 nm ($A_{417}$) as a function of time. The inset in panel C follows $A_{414}$ and $A_{405}$ as a function of time to monitor the decay of oxy-DHP and rise of ferric DHP, respectively. The bold lines on the traces show exponential fits for the indicated time ranges, which yield calculated apparent first-order rate constants of $4.7 \times 10^{-2}$ $s^{-1}$ from $A_{414}$ and $1.0 \times 10^{-2}$ $s^{-1}$ from $A_{405}$.

values (equilibrium) for DHP,[3] and in this study, we observed no significant difference in the $k_{d(O_2)}$ values (kinetics) measured in the absence and presence of TCP (1 mM) (Figure S3 of the Supporting Information). These results rule out the possibility that TCP triggers the functional switch by attenuating $O_2$ binding.[26] In addition, we have shown clear evidence that blocking the catalytic activity of the ferric component in the oxy-DHP sample (using ferric heme ligands, Im and cyanide) also blocks the functional switch, and such blockage by Im can be reversed by HRP (Figure 4A) that catalyzes the oxidation of

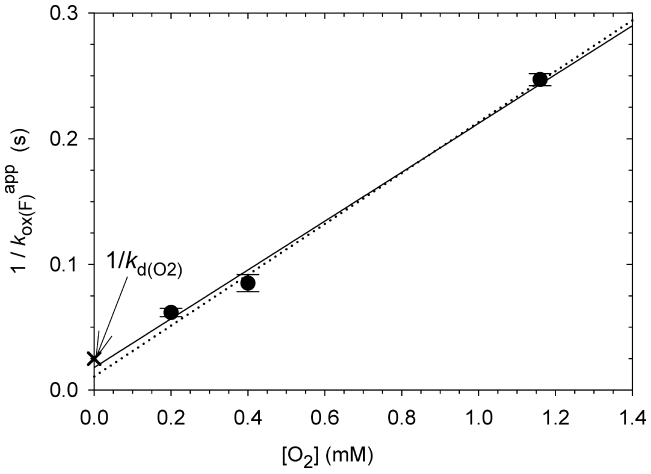


**Figure 8.** Plot of $1/k_{ox(F)}^{app}$ [$k_{ox(F)}^{app}$ is the apparent rate constant for oxidation of oxy-DHP with 1 mM ferricyanide] vs $O_2$ concentration (0.20, 0.40, and 1.16 mM) (●). The times sign on the *Y*-axis is $1/k_{d(O_2)}$ [$k_{d(O_2)}$ is the rate constant for dissociation of $O_2$ from oxy-DHP]. The straight lines are linear fits for the three [without the *Y*-intercept point (×) (···)] or all four points (—).

the substrate TCP to its radical.[13,14] Previously, a spin-trapping reagent DIPPMO (5-diisopropoxy-phosphoryl-5-methyl-1-pyrroline-*N*-oxide) has been reported to trap the TCP$^•$ generated from the reaction of ferric DHP or oxy-DHP with $H_2O_2$ in the presence of TCP as demonstrated by $^{31}$P nuclear magnetic resonance.[26] However, the identity of the compound formed by the trapping was not established, and the possible inhibition of oxy-DHP to ferric DHP or ferryl DHP conversion by DIPPMO was not examined in that study. In the study presented here, we have used DMPO as the TCP radical trap to probe the role of TCP in triggering the DHP functional switch. The complete inhibition of the TCP/4-BP-triggered (but not the ferrocyanide-triggered) activation of oxy-DHP by DMPO observed at <50 $\mu$M $H_2O_2$ confirms the involvement of TCP radicals in the DHP functional switch under these conditions.

On the basis of the results from this study for the activation of oxy-DHP as well as our previous findings,[25] shown in Scheme 2, we illustrate the mechanism for the $H_2O_2$-mediated oxidation of oxy-DHP to the ferric state in the presence of substrate TCP (as proposed previously[25]) or ferrocyanide (newly found in this study). In the first phase, oxyferrous DHP is oxidized to ferric DHP by TCP$^•$ or ferricyanide (with bimolecular rate constant $k_1$ or $k_1^{app}$), where $k_1$ or $k_1^{app}$ denotes the rate constants for ferrous DHP in the absence or presence of $O_2$, respectively (i.e., $k_1^{app}$ is an $O_2$ concentration-dependent value). Both ferric DHP and TCP$^•$ are the oxidative products gradually generated from the normal peroxidase catalytic cycle mediated by the initial trace amount of ferric DHP present in the oxy-DHP sample. It is most likely that TCP radical oxidizes oxy-DHP via the deoxyferrous form as shown for the oxidation of oxy-Mb[40]and oxy-DHP (Figure 8) by ferricyanide. This proposal is based on the very similar and parallel $O_2$ concentration-dependent behaviors of TCP and ferrocyanide in their role(s) in the oxidative conversion of oxy-DHP to ferric or ferryl DHP (Table 3). Varying the $O_2$ concentration can shift the equilibrium between $O_2$-bound and free ferrous forms of DHP. Under such conditions, changes in the concentrations (fractions) of deoxyferrous DHP would more significantly depend on $O_2$ concentration (for example, 0.2 mM vs 0.4 mM)


dx.doi.org/10.1021/bi5002757 | *Biochemistry* 2014, 53, 4956−4969

**Scheme 2. Proposed Reaction Mechanism for $H_2O_2$ Converting Oxy-DHP to the Ferric State in the Presence of TCP (green) or Ferrocyanide (pink) (pathway A) and an Alternative Mechanism for $H_2O_2$ Oxidizing Deoxyferrous DHP to the Ferryl State (Cpd II) (pathway B) Shown as a Thick Dotted Line (dark pink)[a]**

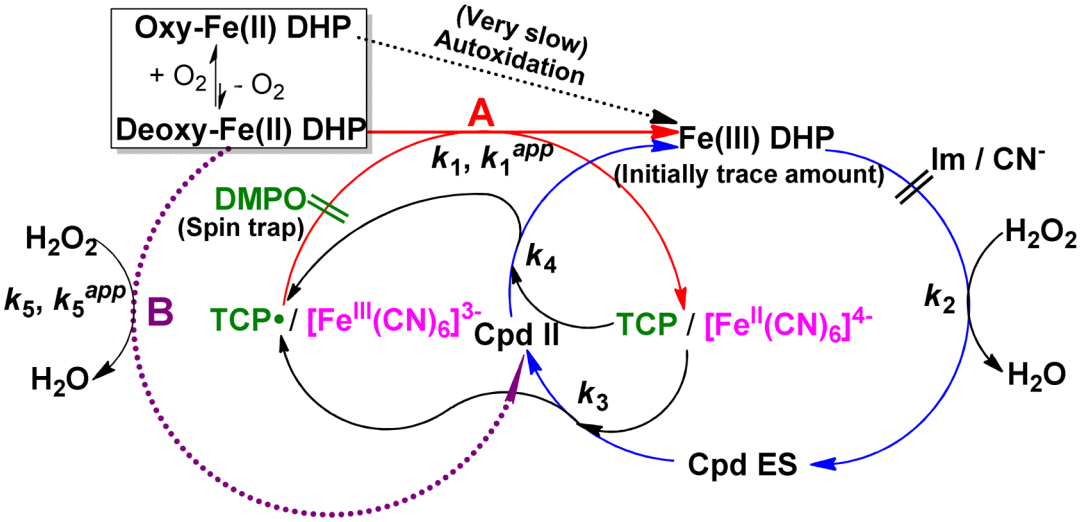


[a]In addition a very slow autoxidation of oxy-DHP to ferric state is indicated by thin dotted line (black).

because the fractions of oxy-DHP will not change significantly because of the fairly low $K(O_2)$ value ($3.2 \times 10^{-6}$ M);[3] in fact, the fraction of oxy-DHP changes only from ~99.2% [=400/(400 + 3.2) at 0.40 mM $O_2$] to ~98.4% [200/(200 + 3.2) at 0.20 mM $O_2$], by <1% [(99.2 − 98.4)/99.2 ~ 0.008], while the deoxyferrous DHP concentration increases from ~0.8 to ~1.6% (by ~100%). Furthermore, even though we propose that deoxyferrous DHP is the actual species that is directly oxidized with TCP• [as with ferricyanide (Figure 8)], such a reaction would be spectrally observed as conversion of oxy-DHP to ferric DHP due to the very low fractional presence of the deoxyferrous form relative to oxy-DHP.

In another conversion pathway, oxy-DHP autoxidizes very slowly (shown by the black dotted line in the middle top part of Scheme 2) and the reaction was accelerated ~3-fold by the addition of TCP (10 $\mu$M) to give a $t_{1/2}$ value of ~24 h at pH 7.0 and ~20 °C.[25] TCP radicals that are likely to be generated by a mechanism identical to the TCP-triggered oxidation of oxy-DHP may accelerate the autoxidation. In the autoxidation reaction, $H_2O_2$ is probably produced by aerobic autoxidation of TCP.

In the second phase (Scheme 2), the oxy-DHP-converted ferric state is oxidized to ferryl DHP upon reacting with $H_2O_2$ (with bimolecular rate constant $k_2$). In the following third/fourth phases, the ferryl DHP species (Cpd ES and Cpd II) decay to Cpd II and ferric DHP, respectively, with bimolecular rate constants $k_3$ and $k_4$, respectively. This is the stage when TCP or ferrocyanide (the product of oxidation of oxy-DHP by TCP• or ferricyanide) reduces ferryl DHP back to the ferric state. The values of the bimolecular rate constants ($k_1^{app}$) for ferricyanide (which is dependent on $O_2$ concentration), $k_2$, and $k_4$ have been determined in this study using a stopped-flow technique and are listed in Table 4. The $k_1$ value is a calculated rate constant for the oxidation of deoxyferrous DHP by ferricyanide that was obtained in this study (Figure 8, *vide infra*). Determination of $k_3$ is not technically feasible because DHP Cpd ES and Cpd II are spectrally indistinguishable. Assuming $k_3 > k_4$, the rate constants that have been determined in this study for Cpd ES + TCP/ferrocyanide reflect the $k_4$ value instead of the $k_3$ value. D'Antonio and Ghiladi have reported the bimolecular rate constant for the reaction of ferryl DHP B with TCP to be $4.1 \times 10^2$ $M^{-1}$ $s^{-1}$ at pH 8 and 25 °C.[26] This value is on the same order of magnitude as the $k$ value (presumably $k_4$) obtained in this study for DHP A (Cpd ES + TCP) at pH 7 and 4 °C (Table 4). In the case of HRP, we have shown in a previous study that $k_3 \sim 3 \times 10^7$ $M^{-1}$ $s^{-1}$ $\gg k_4 \sim 1.5 \times 10^5$ $M^{-1}$ $s^{-1}$ for ferryl HRP oxidation of TCP at pH 5.[34] An upper estimate for $k_5$ for oxidation of deoxyferrous DHP by $H_2O_2$ is used on the basis of the value ($1.60 \times 10^3$ $M^{-1}$ $s^{-1}$) determined for DHP B at room temperature and pH 8.0 by D'Antonio and Ghiladi.[26] The $k_5$ value should change depending on $O_2$ concentration and will be denoted as $k_5^{app}$ under nonanaerobic conditions.

As shown in Scheme 2, ferric DHP ligands (Im and $CN^-$) effectively inhibit the functional switch by blocking the

**Table 4. Bimolecular Rate Constants for the Reactions Shown in Scheme 2[a]**

| substrate/oxidant | rate constant ($M^{-1}$ $s^{-1}$) at pH 7.0 and 4 °C | |
|---|---|---|
| ferricyanide | $k_1^{app}$ | $(1.8 \pm 0.2) \times 10^4$ |
| ferricyanide | $k_1$[b] | $\sim 1.5 \times 10^6$ |
| $H_2O_2$ | $k_2$ | $(3.5 \pm 0.1) \times 10^4$ |
| TCP | $k_4$ | $(9.4 \pm 0.3) \times 10^2$ |
| 4-BP | $k_4$ | $(9.7 \pm 0.9) \times 10^2$ |
| ferrocyanide | $k_4$ | $(4.4 \pm 0.4) \times 10^2$ |
| $H_2O_2$ | $k_5$[c] | $\sim 5 \times 10^3$ |

[a]$k_1$, $k_2$, and $k_4$ are for the reactions of oxy-DHP with ferricyanide ($k_1^{app}$ in Scheme 2), ferric DHP with $H_2O_2$, and DHP Cpd II with TCP, 4-BP, or ferrocyanide, respectively. Apparent first-order reaction rate constants ($k^{app}$) obtained from the time dependence spectral change of DHP upon reaction with various concentrations of substrates or oxidants (from 1 to 10 equiv) were plotted vs substrate/oxidant concentration, and the bimolecular rate constants ($k_1^{app}$, $k_1$, $k_2$, and $k_4$) were calculated from the linear correlations (see Figure S4 of the Supporting Information for representative examples). [b]Estimated value obtained in this study (see Figure 8 and the text). [c]Upper estimated value based on the value ($1.6 \times 10^3$ $M^{-1}$ $s^{-1}$) reported for DHP B at pH 8.0 and 20 °C.[26]


dx.doi.org/10.1021/bi5002757 | *Biochemistry* 2014, 53, 4956−4969

formation of Cpd ES and thus the generation of subsequent oxidative products, TCP$^{\bullet}$ or $[Fe^{III}(CN)_6]^{3-}$. DMPO inhibits the functional conversion (TCP-triggered only) by trapping the TCP$^{\bullet}$ that oxidizes oxy-DHP to the ferric state. In the absence of these inhibitors, this reaction cycle continues in an accelerated fashion after the initial slow stage using progressively accumulated ferric DHP and regenerated TCP/ferrocyanide.

In the proposed mechanism described above, oxy-DHP switches to the ferric state without the formation of any intermediate. However, in this study of oxy-DHP to ferric DHP conversion (with an oxy-DHP:$H_2O_2$:substrate concentration ratio of 1:1:1), a ferryl intermediate is formed before the appearance of ferric DHP (Figures 1 and 2B). The apparent inconsistency can be explained using Scheme 2. In the beginning of the activation reaction, TCP$^{\bullet}$ (or ferricyanide) is gradually generated by the peroxidase reaction of $H_2O_2$ (initially 1 equiv) and ferric DHP (initially trace amount). Under such conditions, the concentration of TCP$^{\bullet}$ (or ferricyanide) is much lower than the $H_2O_2$ concentration. Consequently, the apparent rate of the initial oxy-DHP → ferric DHP phase ($k_{obs} = k_1^{app}$[TCP$^{\bullet}$] or $k_1^{app}$[ferricyanide]) is considerably slower than that of the following ferric DHP → Cpd ES phase [$k_{obs} = k_2[H_2O_2] = 3.5 \times 10^4$ M$^{-1}$ s$^{-1}$ × 5 $\mu$M = $1.8 \times 10^{-1}$ s$^{-1}$ (Table 2)]. When the oxy-DHP → ferric DHP phase becomes progressively faster until it reaches its maximal rate [$2.3 \times 10^{-2}$ s$^{-1}$ (TCP) or $4.8 \times 10^{-2}$ s$^{-1}$ (ferrocyanide) (Table 1)], more than half of the initially added $H_2O_2$ remains because 1 equiv of oxy-DHP to ferric DHP conversion requires 1 equiv of TCP$^{\bullet}$ generated by consuming only 0.5 equiv of $H_2O_2$. Therefore, the ferric DHP → Cpd ES phase ($k_{obs} = k_2[H_2O_2] \geq 3.5 \times 10^4$ M$^{-1}$ s$^{-1}$ × 0.5 equiv × 5 $\mu$M = $8.8 \times 10^{-2}$ s$^{-1}$) is still faster than the first oxy-DHP → ferric DHP phase [$k_{obs} = 2.3 \times 10^{-2}$ s$^{-1}$ (Table 1)].

This explains why it is not easy to detect the first phase under the conditions we employed in this study. Actually, what we have observed is a combination of two sequential phases, i.e., oxy-DHP → ferric DHP → Cpd ES DHP, with the former phase being the rate-limiting step. As the consumption of $H_2O_2$ continues while TCP$^{\bullet}$/TCP (or ferricyanide/ferrocyanide) continues to be recycled, the third/fourth phase (ferryl → ferric DHP; $k_{obs} = k_4$[substrate]) becomes dominant over the second phase (ferric DHP → Cpd ES; $k_{obs} = k_2[H_2O_2]$) and the ferryl intermediate starts to be reduced back to the ferric state. Thus, ferric DHP produced in the first phase is partially converted to ferryl DHP (~45%, as shown by the global analysis in Figure 1B) and then generated an ~100% stoichiometric amount at the end of the reaction.

However, when excess TCP is used as in our previous study[25] (oxy-DHP:$H_2O_2$:TCP concentration ratio of 1:1:30), the rate of the third/fourth phases (ferryl → ferric DHP; $k_{obs} = k_4$[TCP] = $9.4 \times 10^2$ M$^{-1}$ s$^{-1}$ × 150 $\mu$M = $1.4 \times 10^{-1}$ s$^{-1}$) exceeds the apparent ferryl DHP formation rate [$k_{obs} = 2.3 \times 10^{-2}$ s$^{-1}$ (Table 1)]. As a result, the ferryl species was not detectable and only two species, oxy-DHP and Fe(III) DHP, were observed during the activation reaction with a single set of isosbestic points.

The first step (oxy-DHP → ferric DHP) in the activation reaction was not detectable in either of the cases described above. However, it could be detected when sufficiently high concentrations of oxidant (TCP$^{\bullet}$ or ferricyanide) of oxy-DHP are available. In fact, such a situation was observed in the reaction of oxy-DHP with an equal number of equivalents of the oxidant ferricyanide and $H_2O_2$ (Figure 4), in which the $k_{obs}$ of the first step (0.09 s$^{-1}$) is actually slower than that of the second step (0.18 s$^{-1}$), as calculated from the bimolecular rate constants $k_1$ and $k_2$ in Table 4 under the conditions employed. However, because no Fe(III) DHP is present at the start of the reaction, we have observed a first phase [0−5 s (Figure 2B, bottom panel)] during which ferricyanide oxidizes oxy-DHP partially to the ferric state (blue triangles), which subsequently forms ferryl DHP upon reacting with $H_2O_2$ (black circles) in the second phase (5−25 s). In the following phase [25−300 s (Figure 4B, top panel)], ferryl DHP slowly decays (0.008 s$^{-1}$, black circles) along with an increase (absorption decrease) for ferric DHP (0.008 s$^{-1}$, blue triangles). This is a process indicated in Scheme 2 as the third/fourth phases when ferrocyanide (recycled from oxy-DHP reducing ferricyanide) is reducing ferryl DHP to the ferric state.

As already mentioned earlier, a "lag" (slow phase) time of ~25 s has been found before the ferryl DHP formation rate reaches its maximum (Figure 1A, right panel inset). This observation is reasonable if we consider that the conversion reaction starts from a trace amount of Fe(III) DHP catalyzing the formation of TCP$^{\bullet}$ and is accelerated until it reaches its maximal rate. On the other hand, direct oxidation of deoxyferrous DHP (in equilibrium with the oxy form) by $H_2O_2$, as proposed by Ghiladi and co-workers, will not explain such a lag period, in contrast to the case of the reaction of oxy-Mb with $H_2O_2$, where no such lag phase is observed.[41] Furthermore, such direct oxidation of deoxyferrous DHP to the ferryl state by $H_2O_2$ would not be inhibited by the ferric heme ligands, Im or $CN^-$. Taken together, the ferryl intermediate observed in the $H_2O_2$-mediated oxy-DHP to ferric DHP conversion is more likely derived from $H_2O_2$ subsequently reacting with the initially generated ferric DHP, not from $H_2O_2$ directly reacting with ferrous DHP.

Although we have provided convincing evidence that supports our original proposal suggesting the involvement of the substrate TCP radical in the functional conversion of oxy-DHP to ferric DHP, we consider a likely additional or alternative mechanism(s) that could compete with the radical mechanism. In particular, oxidation of deoxyferrous DHP to ferryl enzyme by $H_2O_2$ is a possible pathway for the functional conversion for DHP as recently proposed by D'Antonio and Ghiladi.[26] In fact, such a reaction of deoxyferrous heme proteins (such as Mb,[41] leghemoglobin,[42] and cytochrome *c* peroxidase[43]) with $H_2O_2$ is well-known. It should be pointed out, however, that the substrate TCP has little effect on the $O_2$ binding equilibrium (affinity) or the kinetics of $O_2$ complex formation as demonstrated in our previous study and this study, especially at a concentration as low as 5 $\mu$M. In addition, in the absence of substrate (TXP), oxy-DHP is converted to Cpd RH-like species, not to ferryl DHP, by addition of >1 equiv of $H_2O_2$.[25] Thus, we consider only the reaction of a small fraction of deoxyferrous DHP with $H_2O_2$ in the presence of substrate (TXP).

Deoxyferrous DHP is in substrate-independent equilibrium with oxyferrous DHP under air. The bimolecular rate constant for the oxidation of deoxyferrous DHP by $H_2O_2$ has been reported by D'Antonio and Ghiladi[26] to be on the order of $10^3$ M$^{-1}$ s$^{-1}$ ($1.60 \times 10^3$ M$^{-1}$ s$^{-1}$) at room temperature and pH 8.0 for DHP B. Assuming that DHP A has similar rate constants at pH 7.0 (even though we used 4 °C in our current study) and taking an upper estimate for the rate constant [using a notation of $k_{ox(H_2O_2)}$] of $5 \times 10^3$ M$^{-1}$ s$^{-1}$, we can estimate the ferrous


dx.doi.org/10.1021/bi5002757 | *Biochemistry* 2014, 53, 4956−4969

(deoxy and oxy) DHP to ferryl DHP conversion rates under 1 atm of air (~0.40 mM $O_2$ at 4 °C). Because such conversion rates are dependent on $O_2$ concentration (i.e., on the fractions of the deoxyferrous form in the largely oxyferrous form of DHP) in solution as is the case of ferricyanide oxidation of oxy-DHP shown and described in detail in this paper, we can estimate the apparent rate constant by using an imaginary plot for $1/k_{ox(H_2O_2)}$ versus $O_2$ concentration analogous to Figure 8. By calculation, we can obtain the following equation at a given $O_2$ concentration, i.e., under a given temperature and atmospheric pressure (see footnote a of the Supporting Information for detailed calculations).

$$k_{ox(H_2O_2)}^{app} \sim 0.016[H_2O_2]/[O_2]\ (s^{-1})$$

Thus, $k_{ox(H_2O_2)}^{app}$ at 4 °C under 1 atm of air (0.40 mM $O_2$) would be 0.004, 0.008, and 0.04 $s^{-1}$ at 0.1, 0.2, and 1 mM $H_2O_2$, respectively. For comparison, the experimental rate constants for oxidation of oxy-DHP (5 $\mu$M) with 0.05−0.2 mM $H_2O_2$ in the presence of 5 $\mu$M TCP are ~0.027 $s^{-1}$ (see Table 2 and Figure 4A). Therefore, these estimated $k_{ox(H_2O_2)}^{app}$ values suggest that the pathway of $H_2O_2$ oxidation of deoxyferrous DHP (pathway B in Scheme 2) under these conditions (1 atm of air and 4 °C) may be able to compete with the TCP radical mechanism (pathway A in Scheme 2) at $10^{-3}$ M (millimolar) $H_2O_2$. However, a higher $H_2O_2$ concentration requires higher substrate (TXP) concentration (>5 $\mu$M) to prevent "Cpd RH" formation (see Figure 4A); as a consequence of increasing $H_2O_2$ and TCP concentrations, more $TCP^{\bullet}$ would be formed, and thus, the $TCP^{\bullet}$-mediated conversion rate would also increase. Furthermore, at <0.2 mM $H_2O_2$, the radical pathway becomes predominant. The lack of $H_2O_2$ concentration dependence of the conversion rate between 0.05 (10 equiv) and 0.2 mM (40 equiv) $H_2O_2$ (Table 2) supports this assessment. In fact, at <50 $\mu$M $H_2O_2$, pathway B in Scheme 2 is virtually negligible, and thus, the spin trap DMPO can effectively inhibit the conversion as demonstrated in this study.

When the $O_2$ concentration is much lower (as low as <5% of the normal value of ~260 $\mu$M at ~20 °C) and the $O_2$ binding equilibrium is largely shifted toward the deoxyferrous form, pathway B could become competitive with the radical mechanism. On the other hand, at lower $O_2$ concentrations, the radical-mediated conversion rate also becomes faster (Table 3). In essence, the large difference (by a factor of ~$10^3$) in the intrinsic bimolecular rate constants for the oxidation of deoxyferrous DHP by $TCP^{\bullet}$ and $H_2O_2$ ($k_1$-equivalent and $k_5$, respectively, in Scheme 2 and Table 4) appears to be the main factor favoring radical pathway A over direct $H_2O_2$-mediated oxidation pathway B in Scheme 2. Besides, millimolar concentrations of $H_2O_2$ themselves may be detrimental to the DHP heme protein because of its highly oxidizing and reactive oxygen species-generating nature.[44] Furthermore, the existence of such extremely low $O_2$ concentrations (for example, <0.05 atm of air) when it is necessary to remove the toxicity of TXP may be unusual in the environment of this organism. Considering these factors, the significant involvement of a functional switch by direct oxidation of deoxyferrous DHP by $H_2O_2$ to ferryl DHP under a typical oxygen atmosphere seems improbable.

## CONCLUSIONS

In this report, we have shown that the DHP functional switch from the oxyferrous state to the ferric peroxidase active state, triggered by the copresence of the substrate TCP and $H_2O_2$, is inhibited by the ferric heme ligands Im and cyanide as well as by the radical trap DMPO. These results and the $O_2$ concentration dependence of the conversion rates observed in this study strongly support our previous proposal that the oxyferrous enzyme is oxidized to the ferric state by TCP radicals via the deoxyferrous form as suggested by this study. The TCP radicals are generated by the peroxidase reaction of ferric DHP that is initially present in a trace amount in the oxy-DHP sample and progressively accumulating. On the other hand, we have shown that TCP-induced displacement of bound $O_2$ followed by $H_2O_2$ binding as proposed by D'Antonio and Ghiladi[26] and recently reviewed by Franzen et al.[45] is unlikely. Direct oxidation of deoxyferrous DHP by $H_2O_2$ to the ferryl state can occur;[26] however, such a functional conversion pathway for DHP under air and normal physiological conditions appears far from being competitive with the mechanism involving TCP radicals. This report further clarifies how this bifunctional $O_2$ carrier hemoglobin switches to its enzymatically active ferric state as a defensive response to the presence of toxic trihalophenol substrates.

## ASSOCIATED CONTENT

### Supporting Information

Overlaid spectra of oxyferrous DHP, ferric DHP, and Cpd ES DHP and simulated spectra for a mixture of these three species using the global analysis data for their time-dependent relative populations shown in Figure 1B (Figure S1), mass spectrum of the 4-BP-DMPO adduct product (Figure S2), stopped-flow rapid scan UV−visible spectroscopic monitoring upon reaction of 20 mM sodium dithionite with 5 $\mu$M oxy-DHP (concentrations after mixing) for a period of 0−0.1 s in the absence (A) and presence of 1 mM TCP (B) (Figure S3), measurements of the apparent ($O_2$ concentration-dependent) bimolecular rate constants $k_1^{app}$ (ferricyanide oxidation of oxy-DHP) and $k_2$ (formation of Cpd ES upon oxidation of ferric DHP by $H_2O_2$) (Figure S4). This material is available free of charge via the Internet at http://pubs.acs.org.

## AUTHOR INFORMATION


### Corresponding Authors

*Department of Chemistry and Biochemistry, 631 Sumter St., University of South Carolina, Columbia, SC 29208. E-mail: msono@mailbox.sc.edu. Phone: (803) 576-5773. Fax: (803) 777-9521.

*Department of Chemistry and Biochemistry, 631 Sumter St., University of South Carolina, Columbia, SC 29208. E-mail: jdawson@mailbox.sc.edu. Phone: (803) 777-7234. Fax: (803) 777-9521.

### Present Address

§J.D.: Yale University School of Medicine, Yale University, New Haven, CT 06510.



### Funding

This project was supported by National Science Foundation Grant MCB 0820456.


### Notes

The authors declare no competing financial interest.

## ■ ACKNOWLEDGMENTS

We thank Prof. Lukasz Lebioda and Dr. Mike Walla (Department of Chemistry and Biochemistry, University of South Carolina) for helpful discussions and Prof. Stefan Franzen (North Carolina State University, Raleigh, NC) for the six-His-tagged DHP plasmid. We also thank one of the anonymous reviewers for suggesting the $O_2$ concentration dependence experiments for the oxy-DHP to ferric or ferryl DHP conversion with ≥1 equiv of $H_2O_2$ in the presence of TCP/ferrocyanide (1 equiv), which provided useful insights into the reaction mechanisms for the functional switching of DHP.

## ■ ABBREVIATIONS

DHP, dehaloperoxidase; Mb, myoglobin; HRP, horseradish peroxidase; CPO, *Caldariomyces fumago* chloroperoxidase; TXP, 2,4,6-trihalophenol; DXQ, 2,6-dihaloquinone; TCP, 2,4,6-trichlorophenol; TCP$^{\bullet}$, TCP radical or one-electron-oxidized TCP; 4-BP, 4-bromophenol; Cpd I, Compound I; Cpd II, Compound II; Cpd ES, Compound ES (common name for Cpd II/Tyr radical); Cpd III, Compound III; Cpd RH, DHP heme species formed upon decays of Cpd ES or reactions of oxy-DHP with excess equivalent amounts of $H_2O_2$, both in the absence of substrate (TXP); DMPO, 5,5-dimethyl-1-pyrroline-*N*-oxide.

## ■ REFERENCES

(1) Han, K., Woodin, S. A., Lincoln, D. E., Fielman, K. T., and Ely, B. (2001) *Amphitrite ornata*, a marine worm, contains two dehaloperoxidase genes. *Mar. Biotechnol. 3*, 287−292.

(2) Weber, R. E., Mangum, C., Steinman, H., Bonaventura, C., Sullivan, B., and Bonaventura, J. (1977) Hemoglobins of two terebellid polychaetes: *Enoplobranchus sanguineus* and *Amphitrite ornata*. *Comp. Biochem. Physiol., Part A: Mol. Integr. Physiol. 56*, 179−187.

(3) Sun, S., Sono, M., Wang, C., Du, J., Lebioda, L., and Dawson, J. H. (2014) Influence of heme environment structure on dioxygen affinity for the dual function *Amphitrite ornata* hemoglobin/dehaloperoxidase. Insights into the evolutional structure-function adaptations. *Arch. Biochem. Biophys. 545*, 108−145.

(4) Osborne, R. L., Taylor, L. O., Han, K. P., Ely, B., and Dawson, J. H. (2004) *Amphitrite ornata* dehaloperoxidase: Enhanced activity for the catalytically active globin using MCPBA. *Biochem. Biophys. Res. Commun. 324*, 1194−1198.

(5) Chen, Y. P., Woodin, S. A., Lincoln, D. E., and Lovell, C. R. (1996) An unusual dehalogenating peroxidase from the marine terebellid polychaete *Amphitrite ornata*. *J. Biol. Chem. 271*, 4609−4612.

(6) Osborne, R. L., Coggins, M. K., Raner, G. M., Walla, M., and Dawson, J. H. (2009) The mechanism of oxidative halophenol dehalogenation by *Amphitrite ornata* dehaloperoxidase is initiated by $H_2O_2$ binding and involves two consecutive one-electron steps: Role of ferryl intermediates. *Biochemistry 48*, 4231−4238.

(7) Davydov, R., Osborne, R. L., Kim, S. H., Dawson, J. H., and Hoffman, B. M. (2008) EPR and ENDOR studies of cryoreduced compounds II of peroxidases and myoglobin. Proton-coupled electron transfer and protonation status of ferryl hemes. *Biochemistry 47*, 5147−5155.

(8) Davydov, R., Osborne, R. L., Shanmugam, M., Du, J., Dawson, J. H., and Hoffman, B. M. (2010) Probing the oxyferrous and catalytically active ferryl states of *Amphitrite ornata* dehaloperoxidase by cryoreduction and EPR/ENDOR spectroscopy. Detection of compound I. *J. Am. Chem. Soc. 132*, 14995−15004.

(9) Osborne, R. L., Raner, G. M., Hager, L. P., and Dawson, J. H. (2006) *C. fumago* chloroperoxidase is also a dehaloperoxidase: Oxidative dehalogenation of halophenols. *J. Am. Chem. Soc. 128*, 1036−1037.

(10) Osborne, R. L., Coggins, M. K., Terner, J., and Dawson, J. H. (2007) *Caldariomyces fumago* chloroperoxidase catalyzes the oxidative dehalogenation of chlorophenols by a mechanism involving two one-electron steps. *J. Am. Chem. Soc. 129*, 14838−14839.

(11) Kim, S. H., Perera, R., Hager, L. P., Dawson, J. H., and Hoffman, B. M. (2006) Rapid freeze-quench ENDOR study of chloroperoxidase compound I: The site of the radical. *J. Am. Chem. Soc. 128*, 5598−5599.

(12) Roman, R., and Dunford, H. (1972) pH dependence of the oxidation of iodide by compound I of horseradish peroxidase. *Biochemistry 11*, 2076−2082.

(13) Wiese, F., Chang, H., Lloyd, R., Freeman, J., and Samokyszyn, V. (1998) Peroxidase-catalyzed oxidation of 2,4,6-trichlorophenol. *Arch. Environ. Contam. Toxicol. 34*, 217−222.

(14) Sturgeon, B. E., Battenburg, B. J., Lyon, B. J., and Franzen, S. (2011) Revisiting the peroxidase oxidation of 2,4,6-trihalophenols: ESR detection of radical intermediates. *Chem. Res. Toxicol. 24*, 1862−1868.

(15) Osborne, R. L., Coggins, M. K., Walla, M., and Dawson, J. H. (2007) Horse heart myoglobin catalyzes the $H_2O_2$-dependent oxidative dehalogenation of chlorophenols to DNA-binding radicals and quinones. *Biochemistry 46*, 9823−9829.

(16) Du, J., Huang, X., Sun, S., Wang, C., Lebioda, L., and Dawson, J. H. (2011) *Amphitrite ornata* dehaloperoxidase (DHP): Investigations of structural factors that influence the mechanism of halophenol dehalogenation using "peroxidase-like" myoglobin mutants and "myoglobin-like" DHP Mutants. *Biochemistry 50*, 8172−8180.

(17) Roach, M. P., Chen, Y. P., Woodin, S. A., Lincoln, D. E., Lovell, C. R., and Dawson, J. H. (1997) *Notomastus lobatus* chloroperoxidase and *Amphitrite ornata* dehaloperoxidase both contain histidine as their proximal heme iron ligand. *Biochemistry 36*, 2197−2202.

(18) Franzen, S., Roach, M. P., Chen, Y.-P., Dyer, R. B., Woodruff, W. H., and Dawson, J. H. (1998) The unusual reactivities of *Amphitrite ornata* dehaloperoxidase and *Notomastus lobatus* chloroperoxidase do not arise from a histidine imidazolate proximal heme iron ligand. *J. Am. Chem. Soc. 120*, 4658−4661.

(19) Lincoln, D. E., Fielman, K. T., Marinelli, R. L., and Woodin, S. A. (2005) Bromophenol accumulation and sediment contamination by the marine annelids *Notomastus lobatus* and *Thelepus crispus*. *Biochem. Syst. Ecol. 33*, 559−570.

(20) Lovell, C. R., Steward, C. C., and Phillips, T. (1999) Activity of marine sediment bacterial communities exposed to 4-bromophenol, a polychaete secondary metabolite. *Mar. Ecol.: Prog. Ser. 179*, 241−246.

(21) Thompson, M. K., Davis, M. F., De Serrano, V., Nicoletti, F. P., Howes, B. D., Smulevich, G., and Franzen, S. (2010) Internal binding of halogenated phenols in dehaloperoxidase-hemoglobin inhibits peroxidase function. *Biophys. J. 99*, 1586−1595.

(22) Plummer, A., Thompson, M. K., and Franzen, S. (2013) The role of polarity of the distal pocket in the control of inhibitor binding in dehaloperoxidase-hemoglobin. *Biochemistry 52*, 2218−2227.

(23) De Serrano, V., D'Antonio, J., Franzen, S., and Ghiladi, R. A. (2010) Structure of dehaloperoxidase B at 1.58 Å resolution and structural characterization of the AB dimer from *Amphitrite ornata*. *Acta Crystallogr. D66*, 529−538.

(24) LaCount, M. W., Zhang, E., Chen, Y. P., Han, K., Whitton, M. M., Lincoln, D. E., Woodin, S. A., and Lebioda, L. (2000) The crystal structure and amino acid sequence of dehaloperoxidase from *Amphitrite ornata* indicate common ancestry with globins. *J. Biol. Chem. 275*, 18712−18716.

(25) Du, J., Sono, M., and Dawson, J. H. (2010) Functional switching of *Amphitrite ornata* dehaloperoxidase from $O_2$-binding globin to peroxidase enzyme facilitated by halophenol substrate and $H_2O_2$. *Biochemistry 49*, 6064−6069.

(26) D'Antonio, J., and Ghiladi, R. A. (2011) Reactivity of deoxy- and oxyferrous dehaloperoxidase B from *Amphitrite ornata*: Identification of compound II and its ferrous−hydroperoxide precursor. *Biochemistry 50*, 5999−6011.

(27) Cai, D., and Tien, M. (1992) Kinetic studies on the formation and decomposition of compounds II and III. Reactions of lignin peroxidase with $H_2O_2$. *J. Biol. Chem. 267*, 11149−11155.
(28) Barr, D. P., and Aust, S. D. (1994) Conversion of lignin peroxidase compound III to active enzyme by cation radicals. *Arch. Biochem. Biophys. 312*, 511−515.
(29) Dunford, H. B. (1999) *Heme peroxidases*, John Wiley, New York.
(30) Belyea, J., Gilvey, L. B., Davis, M. F., Godek, M., Sit, T. L., Lommel, S. A., and Franzen, S. (2005) Enzyme function of the globin dehaloperoxidase from *Amphitrite ornata* is activated by substrate binding. *Biochemistry 44*, 15637−15644.
(31) Paul, K. G., Theorell, H., and Akeson, A. (1953) The molar light absorption of pyridine ferroprotoporphrin (pyridine hemochromogen). *Acta Chem. Scand. 7*, 1284−1287.
(32) Nelson, D. P., and Kiesow, L. A. (1972) Enthalpy of decomposition of hydrogen peroxide by catalase at 25 °C (with molar extinction coefficients of $H_2O_2$ solutions in the UV). *Anal. Biochem. 49*, 474−478.
(33) Millero, F. J., Huang, F., and Laferiere, A. L. (2002) Solubility of oxygen in the major sea salts as a function of concentration and temperature. *Mar. Chem. 78*, 217−230.
(34) Sumithran, S., Sono, M., Raner, G. M., and Dawson, J. H. (2012) Single turnover studies of oxidative halophenol dehalogenation by horseradish peroxidase reveal a mechanism involving two consecutive one electron steps: Toward a functional halophenol bioremediation catalyst. *J. Inorg. Biochem. 117*, 316−327.
(35) Thompson, M. K., Franzen, S., Ghiladi, R. A., Reeder, B. J., and Svistunenko, D. A. (2010) Compound ES of dehaloperoxidase decays via two alternative pathways depending on the conformation of the distal histidine. *J. Am. Chem. Soc. 132*, 17501−17510.
(36) Antonini, E., and Brunori, M. (1971) *Hemoglobin and myoglobin in their reactions with ligands*, Chapter 2, North-Holland Publishing Co., Amsterdam.
(37) Du, J., Sono, M., and Dawson, J. H. (2008) The proximal and distal pockets of the H93G myoglobin cavity mutant bind identical ligands with different affinities: Quantitative analysis of imidazole and pyridine binding. *Spectroscopy 22*, 123−141.
(38) Ellis, W. D., and Dunford, H. B. (1968) The kinetics of cyanide and fluoride binding by ferric horseradish peroxidase. *Biochemistry 7*, 2054−2062.
(39) Antonini, E., Brunori, M., and Wyman, J. (1965) Studies on the oxidation-reduction potentials of heme proteins. IV. The kinetics of oxidation of hemoglobin and myoglobin by ferricyanide. *Biochemistry 4*, 545−551.
(40) Wang, C., Lovelace, L. L., Sun, S., Dawson, J. H., and Lebioda, L. (2013) Complexes of dual-function hemoglobin/dehaloperoxidase with substrate 2,4,6-trichlorophenol are inhibitory and indicate binding of halophenol to compound I. *Biochemistry 52*, 6203−6210.
(41) Whitburn, K. D. (1987) The interaction of oxymyoglobin with hydrogen peroxide: The formation of ferrylmyoglobin at moderate excesses of hydrogen peroxide. *Arch. Biochem. Biophys. 253*, 419−430.
(42) Aviram, I., Wittenberg, A., and Wittenberg, J. B. (1978) The reaction of ferrous leghemoglobin with hydrogen peroxide to form leghemoglobin(IV). *J. Biol. Chem. 253*, 5685−5689.
(43) Pond, A. E., Bruce, G. S., English, A. M., Sono, M., and Dawson, J. H. (1998) Spectroscopic study of the compound ES and the oxoferryl compound II states of cytochrome *c* peroxidase: Comparison with the compound II of horseradish peroxidase. *Inorg. Chim. Acta 275*, 250−255.
(44) Alayash, A. I., Patel, R. P., and Cashon, R. E. (2001) Redox reactions of hemoglobin and myoglobin: Biological and toxicological implications. *Antioxid. Redox Signaling 3*, 313−327.
(45) Franzen, S., Thompson, M. K., and Ghiladi, R. A. (2012) The dehaloperoxidase paradox. *Biochim. Biophys. Acta 1814*, 578−588.